JPC 413

Report Number
TM-65-6

Liquid-film Cooling
Its Physical Nature and Theoretical Analysis

by

R. A. Gater
M. R. L'Ecuyer
C. F. Warner

Contract Nonr 1100(21)

October 1965

JET PROPULSION CENTER
PURDUE UNIVERSITY
SCHOOL OF MECHANICAL ENGINEERING
LAFAYETTE, INDIANA

ERRATA SHEET

Page

90 Line 5. ... Eq. 4-21..., should be, ...Eq. 4-23...

90 Equation 4-35 should read:

$$St_{gv} = St_o \frac{t_{aw} - t_w}{t_r - t_w}$$

91 Equation 4-36 should read:

$$St_{gv} = \frac{q_w}{(\rho u)_e c_{p_e} (\bar{t}_r - \bar{t}_w)}$$

97 Reference 36 should read: ...Journal Heat and Mass Transfer, June 1963.

108 The equation on this page should read:

$$189 \text{ psia} \stackrel{?}{=} \frac{500}{1.633 + 1} \text{ psia}$$

$$= 189 \text{ psia}$$

PURDUE UNIVERSITY

AND

PURDUE RESEARCH FOUNDATION

Lafayette, Indiana

Report No. TM-65-6

LIQUID-FILM COOLING, ITS PHYSICAL NATURE AND THEORETICAL ANALYSIS

by

R. A. Gater

M. R. L'Ecuyer

C. F. Warner

Technical Memorandum

Contract Nonr 1100(21)

Jet Propulsion Center

Purdue University

October 1965

ACKNOWLEDGMENTS

The investigation reported herein was conducted under the auspices of the Office of Naval Research, Power Branch, under Contract Nonr 1100 (21).

The subject investigation was conducted under the direction of Dr M. J. Zucrow, Atkins Professor of Engineering. The authors are indebted to Dr. Zucrow for his advice during the preparation and editing of the developments presented herein.

Special appreciation is expressed to Dr. S. N. B. Murthy, formerly Visiting Professor of Mechanical Engineering, Purdue University, for his advice during the initial phase of the investigation.

The authors also wish to express their appreciation to Mr D. L. Crabtree, research assistant, Purdue University, for his suggestions regarding the contents of the subject report.

Thanks is also expressed to Mrs. Joyce Gater for her typing of the original manuscript, and to Mrs. Sandy Lowe for her typing and assistance in the preparation of the final manuscript.

TABLE OF CONTENTS

	Page
LIST OF TABLES	vi
LIST OF FIGURES	vii
ABSTRACT	viii
1. INTRODUCTION	1
1.1 General Discussion	1
1.2 Objectives of the Present Investigation	2
2. THE PHYSICAL NATURE OF LIQUID-FILM COOLING	3
2.1 Description of Liquid-Film Cooling	3
2.1.1 The Liquid-Film-Cooled Region	3
2.1.2 The Gas-Vapor-Cooled Region	13
2.2 Conservation of Mass and Energy at the Gas-Liquid Interface	16
2.2.1 Interfacial Mass Balance	16
2.2.2 Interfacial Energy Balance	22
2.3 Energy Balance on the Liquid Film	25
2.3.1 General Energy Balance	25
2.3.2 Simplified Energy Balances Employed by Previous Investigators	28
2.4 Gas-Liquid Interactions	29
2.4.1 Interfacial Structures	29
2.4.2 Film Instability and Entrainment	33
3. ANALYZING THE LIQUID-FILM-COOLED REGION	41
3.1 A Review of the Previous Analyses	41
3.1.1 The Analyses Due to Kannie, Sellers, Graham, and Knuth	45

Page

3.1 2 The Analysis Due to Emmons 52

3.2 A Review of the Pertinent Experimental Data 55

3.2.1 Heat-Mass Transfer Data 56
3.2 2 Correlation of Velocity Profile Data . . 61

3.3 An Alternate Correlation for Heat-Mass Transfer Data 62

3.3.1 A Method for Predicting the Temperature at the Gas-Liquid Interface 65
3.3.2 Correlation of $(St/St_o)_t$ for Transpiration Cooling 69
3.3.3 A Method for Evaluating St_o 71
3.3.2 Methodology 74

4. AN ANALYSIS FOR THE GAS-VAPOR COOLED REGION 78

4.1 Introduction 78

4.2 The Case Where the Wall is Adiabatic 79

4.2.1 The Flow Model 79
4.2.2 The Energy Balance 81
4.2.3 The Evaluation of m" 85
4.2.4 A Special Case 88

4.3 The Case Where the Wall is Cooled Externally 90

5. CONCLUSIONS AND RECOMMENDATIONS 92

6. BIBLIOGRAPHY 95

APPENDIX A. NOTATION 101

APPENDIX B. A SAMPLE CALCULATION FOR THE INTERFACE TEMPERATURE 106

LIST OF TABLES

Table		Page
1.	A Comparison of the Previous Analyses for Liquid-Film Cooling	42
2.	The Parameters That Are Considered Known as a Function of x in Outlining the Methodology	75

LIST OF FIGURES

Figure		Page
2-1.	A Schematic Representation of the Liquid-Film-Cooling Process	4
2-2.	A Boundary Layer Model for the Liquid-Film Cooled Region	5
2-3.	The Universal "Law of the Wall" for the Turbulent Boundary Layer on a Smooth Surface	8
2-4.	Variation of the Liquid Flow Rate Parameter W^+ with the Dimensionless Film Thickness δ_f^+	11
2-5.	A Schematic Representation of the Pertinent Wall-Temperature Profiles for the Gas-Vapor-Cooled Region	14
2-6.	A Mass-Transfer Interface Element for a Non-Reactive, Stable Liquid Film	16
2-7.	An Energy-Transfer Interface Element for a Stable, Non-Reactive Liquid Film	23
2-8.	Control Volume for Energy Balance on a Stable, Non-Reactive Liquid Film	26
2-9.	Characteristic Interfacial Structures for Liquid-Film Cooling	31
2-10.	The Correlation Due to Graham (10) for the Stability Effectiveness ε_s as a Function of the Liquid Flow Rate Parameter W_o^+	38
3-1.	A Schematic Representation of the Physical Model Employed in the Subject Analyses	46
3-2.	The Temperature at the Interface as a Function of the Static Pressure and the Main-Stream Temperature	67
3-3.	The Correlation for Transpiration Cooling Data Due to Brunner (37)	70
4-1.	The Control Volume for the Gas-Vapor-Cooled Region . .	82

ABSTRACT

A discussion of the physical nature of liquid-film cooling is presented that gives special emphasis to those phenomena occurring at the gas-liquid interface. The interfacial mass and heat balances are discussed in detail, together with the phenomena of film instability and the entrainment of liquid by the gas stream.

A review is presented of the pertinent heat-mass transfer analyses for the wall region wetted by the liquid film. The limitations of those analyses are noted, and an alternate correlation procedure is suggested that is applicable to the case where the gas flow is compressible and subject to the influence of a streamwise pressure gradient. In order to implement that correlation procedure, a method is developed whereby the temperature at the gas-liquid interface can be approximated analytically. Calculated results are presented that are noted to agree favorably with the limited experimental data.

A heat transfer analysis is presented for the wall region downstream of the liquid film. That analysis is based on a relatively simple flow model, and is applicable to the case where the gas flow is compressible and subject to the influence of a streamwise pressure gradient. Two wall conditions are considered: (a) the case where the wall is adiabatic; and (b) the case where the wall is cooled externally.

Conclusions and recommendations for further experimental research are presented.

1. INTRODUCTION

1.1 General Discussion

Liquid-film cooling refers to the injection of a thin continuous liquid film onto a given surface for the purpose of protecting that wetted surface from thermal damage from a hot gas flowing past the film.

The motivation for developing liquid-film-cooling technology for rocket motors has been the development of nuclear rocket engines, the use of higher energy chemical propellants, and the trend toward higher combustion chamber pressures. These newer developments are characterized by a large increase in the heat flux from the working fluid to the walls of the combustion chamber and the exhaust nozzle, such that the regenerative cooling of those walls becomes marginal (1)(2)(3).[1]

A need, therefore, exists for developing a method of cooling which will supplement regenerative cooling. While porous-wall cooling techniques (transpiration cooling which utilizes gaseous coolants and sweat cooling which utilizes liquid coolants) are more effective than liquid-film cooling from the standpoint of the degree of thermal protection realized per pound of coolant consumed, liquid-film cooling still appears to be quite attractive for the following reasons: (a) clogging of the porous wall is still a problem and leads to localized "burnout," (b) a reduction in the structural integrity of large components results

[1] Numbers in parentheses refer to references listed in the Bibliography.

when they are constructed from porous materials, and (c) the fabrication problem is simpler in the case of a liquid-film-cooled system.

Considerable attention has also been devoted to studies concerned with employing a gaseous film coolant Gaseous-film cooling has the same advantage of simplicity as does liquid-film-cooling, but the absence of a phase change during the cooling process severely limits the cooling capacity of gaseous-film cooling in comparison to that of liquid-film cooling

1 2 Objectives of the Present Investigation

The objectives of the subject investigation were threefold:
(a) to describe the physical nature of liquid-film cooling;
(b) to review the theoretical heat-mass transfer correlations for the liquid-film-cooled region, and to develop an alternate correlation for that region; and
(c) to develop a heat transfer correlation for the region downstream of the terminus of the liquid film

The correlation procedures developed herein are generalized so as to be applicable to the flow of a compressible gas in the presence of a streamwise pressure gradient Moreover, the developments consider boundary layer flow rather than fully developed pipe flow, as have previous analyses The developments are limited, however, to the case where the gas flow is fully turbulent and the liquid-film coolant is non-reactive

Assessment of the validity of the correlation procedures developed herein awaits the existence of accurate experimental data. Such experimental work is being conducted currently at the Jet Propulsion Center, Purdue University, Lafayette, Indiana.

2. THE PHYSICAL NATURE OF LIQUID-FILM COOLING

2.1 Description of Liquid-Film Cooling

Figure 2-1 presents a schematic diagram illustrating the pertinent aspects of the liquid-film cooling process. There are two regions of the wall that are of principal interest: (a) the liquid-film-cooled region, and (b) the gas-vapor-cooled region. The phenomena which characterize each of those regions are discussed in the following sections

2.1 1 The Liquid-Film-Cooled Region

Figure 2-2 illustrates a physical boundary layer model for the liquid-film-cooled region The phenomena which relate to the development of that boundary layer region are discussed in the following paragraphs

The Nature of Film Development At station $x = x_0$, in Fig 2-1, the liquid coolant is injected onto the solid surface and establishes a spanwise continuous liquid film The liquid film interacts with and is accelerated by the hot gas stream flowing past it The velocity distribution throughout the liquid film at any streamwise location is determined by the solution of the momentum equation for the two-dimensional flow of an incompressible fluid; the latter can be written in the following form (4) Thus

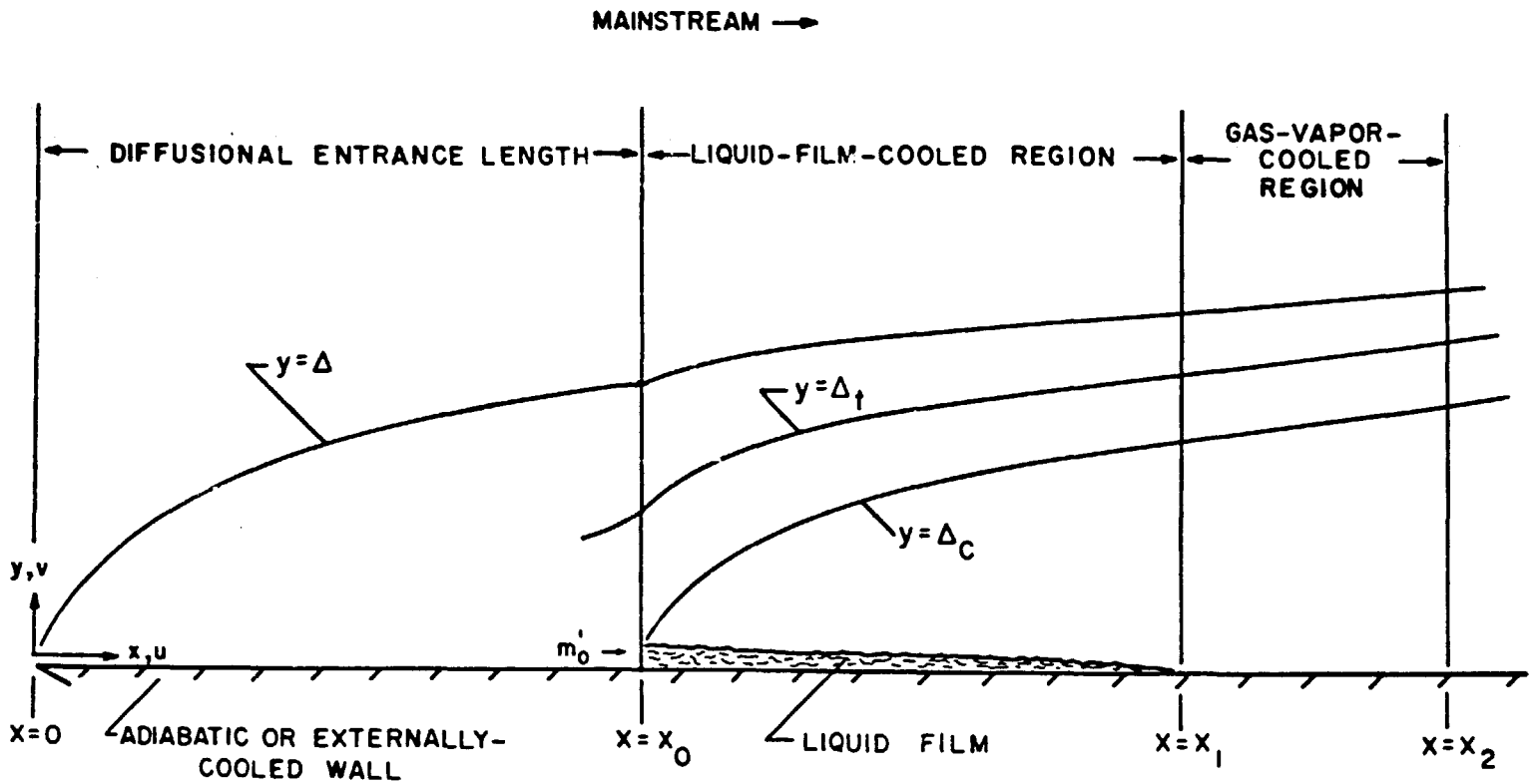

FIG. 2-1. A SCHEMATIC REPRESENTATION OF THE LIQUID-FILM-COOLING PROCESS

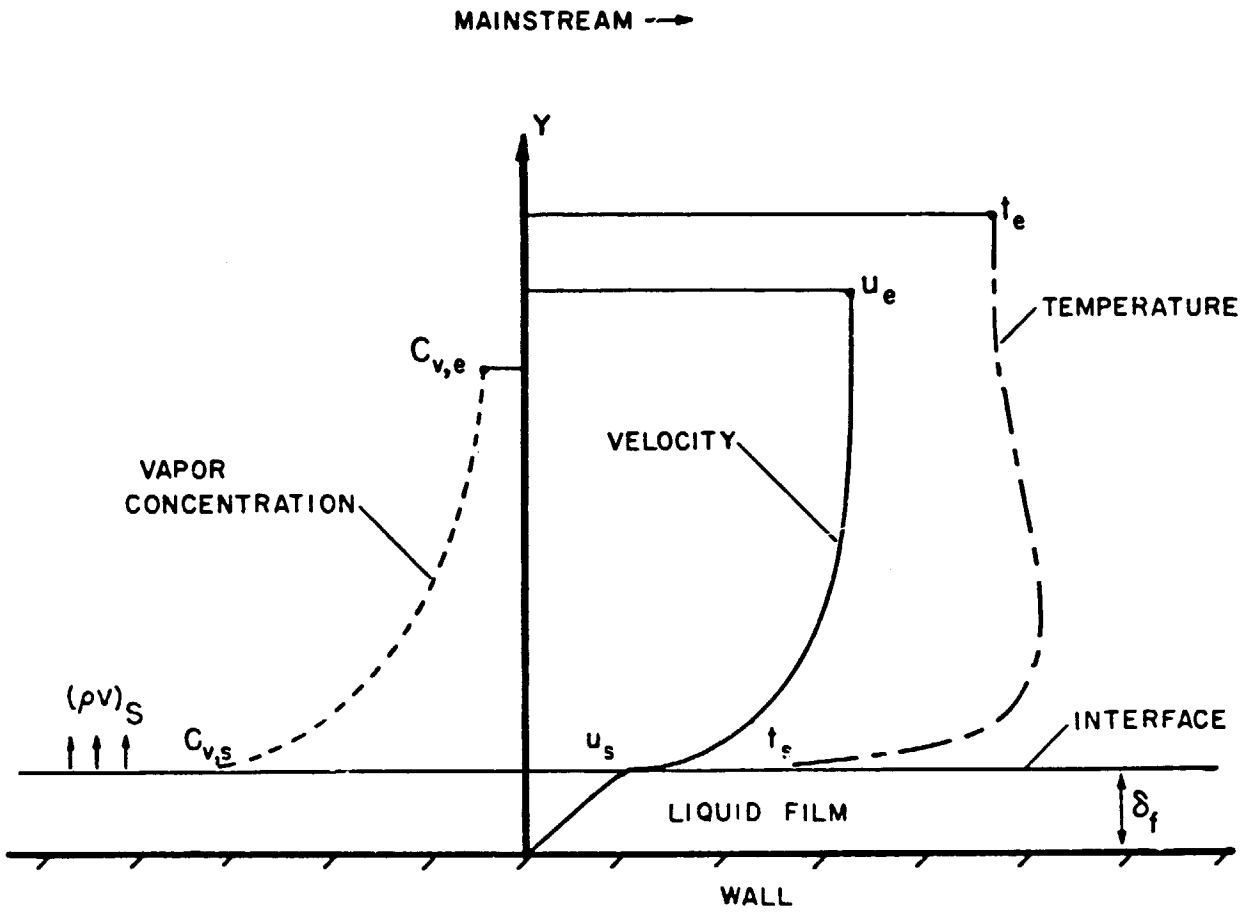

FIG. 2-2. A BOUNDARY LAYER MODEL FOR THE LIQUID-FILM-COOLED REGION

$$\rho_l\left(u\frac{\partial u}{\partial x} + v\frac{\partial u}{\partial y}\right) = -\frac{\partial p}{\partial x} + \frac{\partial \tau}{\partial y} \qquad (2\text{-}1)^1$$

The acceleration terms in Eq. 2-1 are of considerable importance at and near the plane where the liquid is injected. However, for the largest portion of the liquid flow regime, because of the extreme thinness of the liquid film,[2] the acceleration terms and the pressure gradient term in Eq. 2-1 can be considered of negligible importance in comparison to the viscous term. Hence, if τ_s and τ_w denote the shear stress at the gas-liquid interface and at the liquid-solid interface, respectively, then one may write

$$\tau \equiv \rho_l\,(\nu + \nu_t)_l\,\frac{\partial u}{\partial y} = \text{constant} = \tau_s = \tau_w \qquad (2\text{-}2)$$

where ν is the molecular contribution and ν_t is the turbulent or eddy contribution to the "effective" kinematic viscosity. From Eq. 2-2 it follows that the velocity distribution for the liquid film is given by

$$u = \frac{\tau_s}{\rho_l}\int_0^y \frac{dy}{(\nu+\nu_t)_l} \qquad (2\text{-}3)$$

For the special case where the film is entirely laminar ($\nu_t = 0$), Eq. 2-3 reduces to

$$u = \frac{\tau_s}{(\rho\,\nu)_l}\,y \qquad (2\text{-}4)$$

---

[1] Refer to Appendix A for a definition of the notation.

[2] Typical film thicknesses are of the order of 1 to 5 X 10^{-3} in.

The problem of expressing the parameter $(\nu + \nu_t)_l$ as a function of the normal coordinate y, so that the integral term in Eq. 2-3 can be evaluated for the case of a turbulent film, can be circumvented by assuming that the universal "law of the wall" is valid for the liquid-flow regime. Figure 2-3 presents the "law of the wall" in graphical form; the dimensionless parameters u^+ and y^+ presented in the figure are defined as follows:

$$u^+ \equiv \frac{u}{(\tau_s/\rho)^{1/2}} \tag{2-5}$$

$$y^+ \equiv \frac{y\,(\tau_s/\rho)^{1/2}}{\nu} \tag{2-6}$$

Figure 2-3 represents, therefore, a means by which the velocity profile in the liquid film can be prescribed once the value of the interfacial shear stress τ_s is determined; the latter must result from the solution of the momentum equation for the gas-flow regime.

The mass flow rate of liquid per unit spanwise length, denoted by m', and the thickness of the liquid film, denoted by δ_f, are related due to the continuity condition Hence,

$$m' = \rho_l \int_0^{\delta_f} u\, dy \tag{2-7}$$

For the case where the film is totally laminar, Eqs 2-4 and 2-7 can be combined to yield the following expression for the thickness

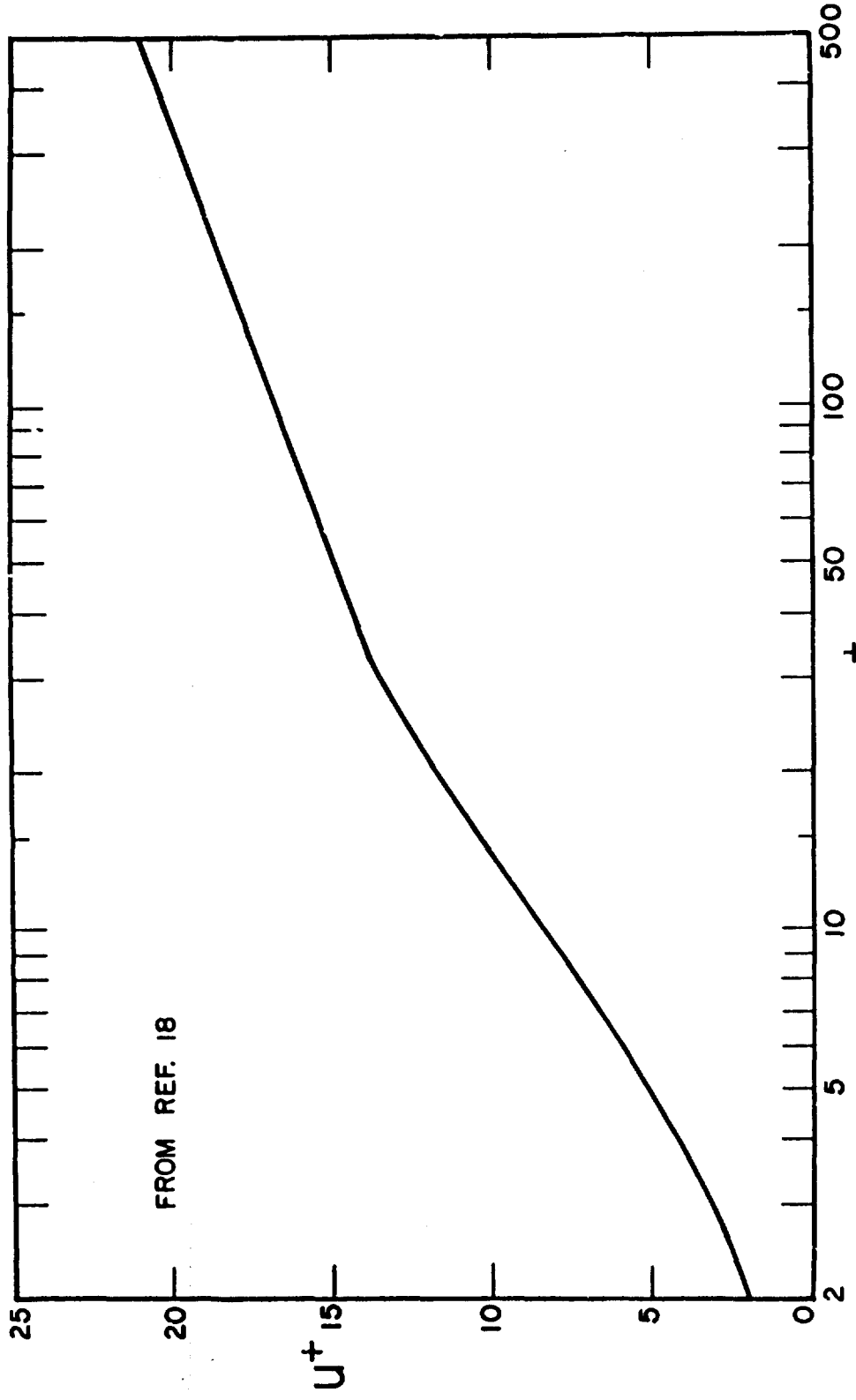

FIG. 2-3. THE UNIVERSAL "LAW OF THE WALL" FOR THE TURBULENT BOUNDARY LAYER ON A SMOOTH SURFACE

of the liquid film:

$$\delta_f = \left[\frac{2m'}{\tau_s/\nu_l}\right]^{\frac{1}{2}} \tag{2-8}$$

To consider the relationship between m' and δ_f for the case where the liquid film is turbulent, it is convenient to rewrite Eq. 2-7 in the following non-dimensional form. Thus

$$W^+ = \int_0^{\delta_f^+} u^+ \, dy^+ \tag{2-9}$$

where the parameter W^+ is termed the dimensionless liquid flow rate, and is defined by

$$W^+ \equiv \frac{m'}{(\rho\nu)_l} \tag{2-10}$$

and where δ_f^+ is the dimensionless film thickness defined by

$$\delta_f^+ \equiv \frac{\delta_f \left(\tau_s/\rho_l\right)^{\frac{1}{2}}}{\nu_l} \tag{2-11}$$

The parameters W^+ and δ_f^+ can be related by employing the "law of the wall," presented in Fig. 2-3, and graphically integrating Eq.2-9.

Figure 2-4 presents W^+ as a function of δ_f^+, as determined by Kinney, et al. (5). The figure illustrates, as does Eq. 2-8, that the thickness of the liquid film is proportional to the liquid flow rate m' and the kinematic viscosity ν_l, and is inversely proportional to the interfacial shear stress τ_s. The significance of the parameter W^+ in determining the physical characteristics of the flow of a thin liquid film is discussed in Section 2.4.

Energy Transfer to the Liquid Film. Energy is transferred to the liquid film from the "hot" gas stream. A small percentage of that energy is utilized for increasing the sensible enthalpy of the liquid in the film. A significant percentage of that energy, however, causes the evaporation of liquid which was raised to its saturation state while flowing downstream.

If the solid surface wetted by the film is thermally insulated from the external environment (i.e., adiabatic), then, after that surface is heated to an equilibrium temperature which is approximately equal to that of the liquid film, all of the incident energy not utilized for increasing the sensible enthalpy of the liquid is utilized to evaporate it. On the other hand, if the solid surface is externally cooled, then a portion of the energy transferred to the liquid film will be transferred through the liquid film and through the solid surface to the external coolant. Thus, with external-regenerative cooling of the solid surface, longer film-cooled lengths will be realized for a given rate of coolant injection than is the case for an adiabatic solid surface.

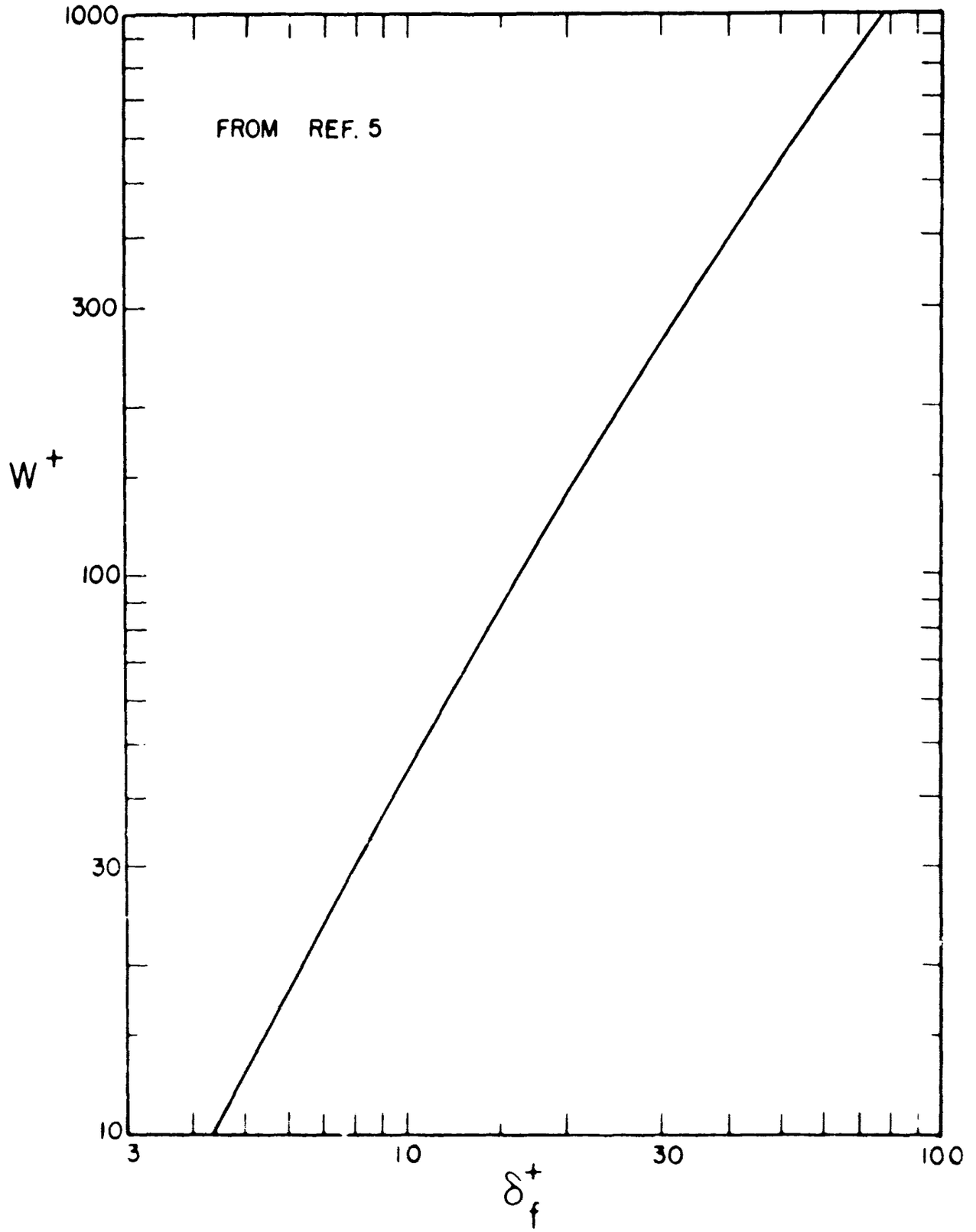

FIG. 2-4. VARIATION OF THE LIQUID FLOW RATE PARAMETER W^+ WITH THE DIMENSIONLESS FILM THICKNESS δ_f^+

Heat Transfer "Blocking." The vapor produced by vaporizing the liquid film coolant is convected and diffused into the boundary layer of the hot gas wetting the liquid film and establishes in turn a concentration (or partial-pressure) boundary layer. In the process of being transported away from the gas-liquid interface, the vapor serves an important function, referred to as the "blocking" of the incident heat flux. In other words, as the vapor moves away from the gas-liquid interface it "absorbs" sensible heat, so that it thus represents a counter-convective heat transfer mechanism.

Film termination. At station $x = x_1$, in Fig. 2-1, the liquid film terminates, due to evaporation and possible entrainment of liquid droplets into the gas stream. An undesirably high degree of droplet entrainment is known to arise when large wave crests, termed disturbances, occur on the surface of the liquid film. The phenomenon of large disturbances on the surface of the film is termed film instability and is discussed in Section 2.4.

Coupling of the Transport Processes and the Boundary Conditions. The interdependence of the heat and mass transfer processes and the related boundary conditions for the evaporation process is illustrated by the following points:

(a) The rate at which energy is transferred to the liquid film and the physical properties of the liquid (particularly its latent heat of vaporization) determine the rate at which vapor is "injected" into the gaseous boundary layer.

(b) The rate of "vapor injection" determines the degree of the aforementioned "blockage" phenomenon and thus the net rate of energy transfer to the liquid film.

(c) The concentration of the vapor at the interface is dependent on the rate at which vapor is introduced into the boundary-layer region (see Section 2.2.1, Eq. 2-23).

(d) The temperature at the interface is determined by the concentration of the vapor at the interface (or, perhaps more correctly, the partial pressure of the vapor at the interface).

(e) The rate at which energy is transferred to the liquid film is dependent on the thermal potential which exists between the main stream and the gas-liquid interface.

The physics of the evaporation process thus require that for a given set of bulk flow conditions (i.e., working fluids, main-stream temperature,pressure, Reynolds number, Mach number, etc.), unique values for each of the following must result: the rate at which energy is transferred to the liquid film; the rate at which liquid is evaporated; and the concentration of the vapor and the temperature at the gas-liquid interface.

2.1.2 The Gas-Vapor-Cooled Region[1]

Figure 2-5 illustrates schematically what is defined as the gas-vapor-cooled region, together with representative profiles of the wall temperature for the cases where the wall is adiabatic and is

[1] The terminology "vapor-cooled region" introduced in Refs. (6) and (7) would appear to be a misnomer in that the quantity of relatively cool gas which exists throughout the boundary layer at $x=x_1$ contributes substantially to the gas-vapor-cooled length.

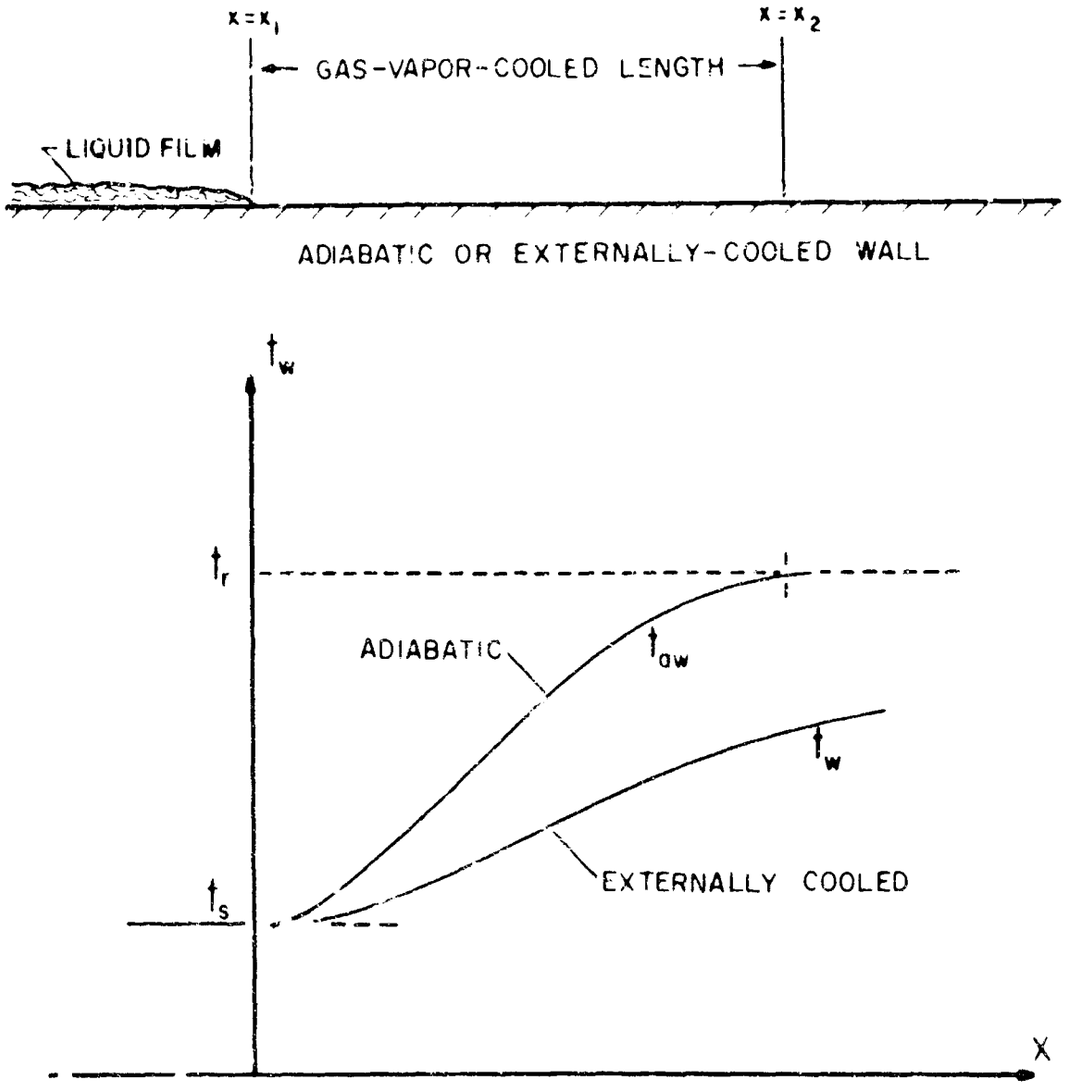

FIG. 2-5. A SCHEMATIC REPRESENTATION OF THE PERTINENT WALL TEMPERATURE PROFILES FOR THE GAS-VAPOR-COOLED REGION

externally cooled The length of the gas-vapor-cooled region, given by x_2-x_1 in the figure, is defined as that in which the temperature of an adiabatic surface, denoted by t_{aw}, increases from the temperature of the liquid film at $x = x_1$, denoted by $t_{s,1}$, to the recovery temperature for the main stream

If the surface downstream from the end of the liquid film is cooled externally, then a wall temperature distribution such as that denoted by t_w in Fig 2-5 results. In general, at any station $x > x_1$, the rate of heat transfer to the external coolant is given by

$$q_w = h'_w (t_{aw} - t_w)$$

where h'_w is the appropriate heat transfer film coefficient to be employed with the thermal potential $(t_{aw} - t_w)$ in the calculation of the wall heat flux q_w To either design an effective regeneratively-cooled downstream region or determine the optimum location for introducing a second liquid-film-cooled region, it must be possible to determine the streamwise distribution of q_w for a prescribed distribution of t_w Hence, the basic problem is that of determining the streamwise distribution of the adiabatic-wall temperature, together with the heat transfer film coefficient h'_w An analysis for the gas-vapor-cooled region is presented in Section 4 which considers those two points.

2.2 Conservation of Mass and Energy at the Gas-Liquid Interface

The conservation of mass and energy across the gas-liquid interface is considered in Sections 2.2.1 and 2.2.2, respectively. Consideration is given only to the case where the liquid film is non-reactive and is stable, free from the consequences of large disturbances (see Section 2.4). It is not assumed that the film is either smooth (free from waviness) or laminar. Moreover, mass diffusion in the boundary layer is treated as a binary process; i.e., the evaporated vapor and the gas entrained from the main stream into the boundary layer are considered as the two counter-diffusing species.

2.2.1 Interfacial Mass Balance

Figure 2-6 illustrates a general interfacial element for mass-transfer, together with the several mass fluxes which are discussed in the following paragraphs. The S- and L-surfaces presented in Fig. 2-6 are defined as being placed in the gas-vapor phase and in the liquid phase, respectively, at an infinitesimal distance from the interface. Additional definitions and subscript notation needed to clarify Fig 2-6 are as follows:

Definitions:

$$(\rho v)_v = \rho_v v_v = \rho_v (v+v_{d,v}) \tag{2-12}$$

$$(\rho v)_g = \rho_g v_g = \rho_g (v+v_{d,g}) \tag{2-13}$$

$$(\rho v) = (\rho_g + \rho_v) v \tag{2-14}$$

$\rho_i \equiv \frac{p_i}{R_i t}$ = the partial density for the "i" species; i=g,v

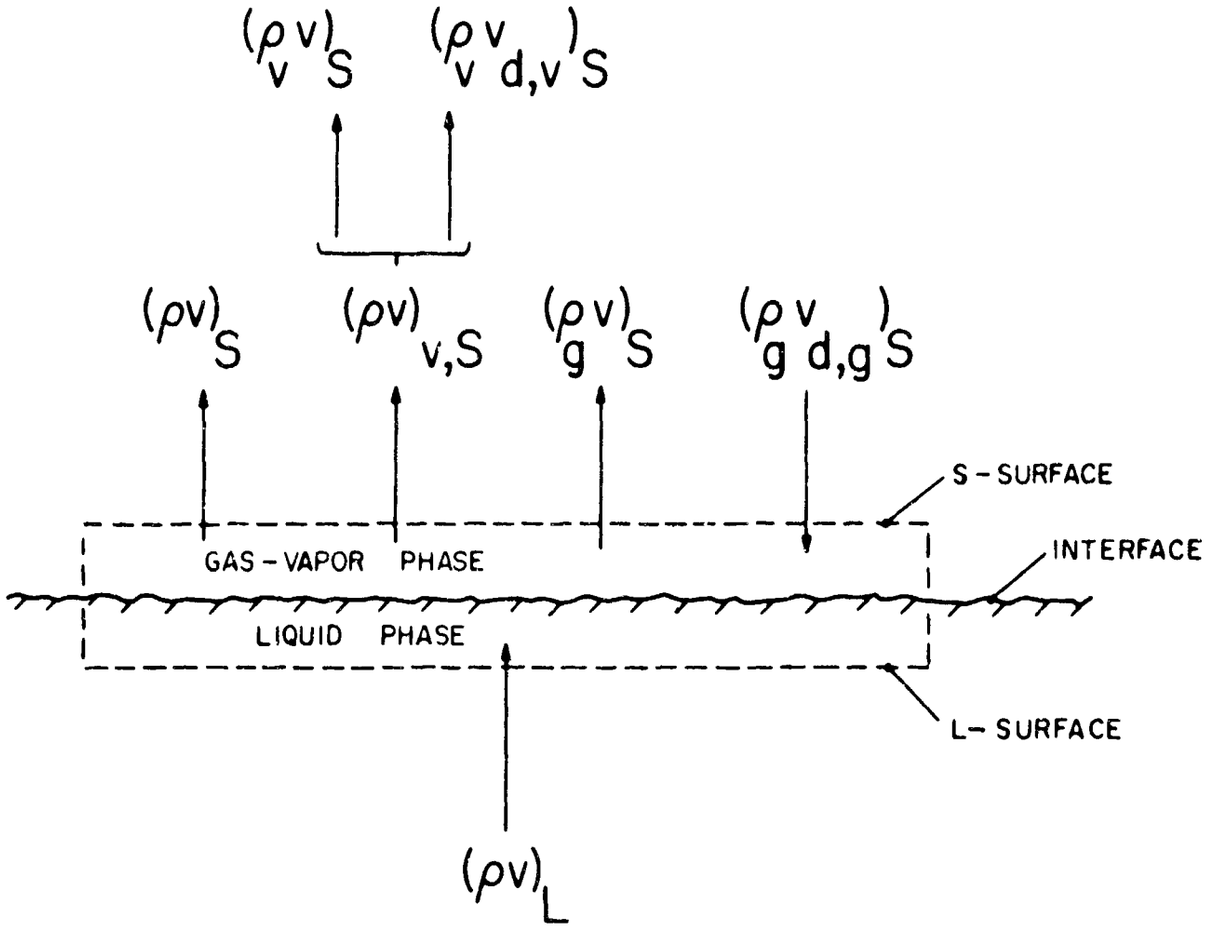

FIG. 2-6. A MASS-TRANSFER INTERFACE ELEMENT FOR A NON-REACTIVE, STABLE LIQUID FILM

p_i = the partial pressure for the "i" species; i=g,v

$\rho = \rho_v + \rho_g$ = the density for the gas-vapor mixture

$v_i = v + v_{i,d}$ = the "total" velocity normal to the S- and L-surfaces for the "i" species; i=g,v

v = the convective velocity normal to the S- and L-surfaces.

$v_{i,d}$ = the diffusional velocity normal to the S- and L-surfaces for the "i" species; i=g,v

Subscripts

v - vapor

g - gas entrained from the main stream

L - evaluated at the L-surface

S - evaluated at the S-surface

d - diffusional component of the subscripted parameter

A term having neither "v," "g" nor "L" as a subscript refers to the gas-vapor mixture

Figure 2-6 illustrates that when the liquid coolant is evaporating into a medium other than its own vapor, mass transport is due to both diffusion and convection. The relationships governing the interdependence of the different convective and diffusive mass fluxes presented in Fig 2-6 are derived in the following paragraphs

Fick's law relates the mass transfer by diffusion in the y direction to the concentration gradient in the y direction, and is expressed by

$$(\rho v_d)_i = -\rho (D + D_t) \left(\frac{\partial C_i}{\partial y}\right) \qquad (i = v,g) \qquad (2\text{-}15)$$

where

$C = \frac{\rho_i}{\rho}$ = the concentration of the "i" species (i = g,v).

$(D + D_t)$ = the "effective" diffusion coefficient

In the case of a binary medium, to which the subject discussion is restricted, the concentration gradients $\partial C_v/\partial y$ and $\partial C_g/\partial y$ are related by

$$\frac{\partial C_v}{\partial y} = - \frac{\partial C_g}{\partial y} \tag{2-16}$$

Equations 2-15 and 2-16 show that at any station y the rates of mass diffusion of the vapor, $(\rho v_d)_v$, and the gas, $(\rho v_d)_g$, are related by

$$(\rho v_d)_g = - (\rho v_d)_v \tag{2-17}$$

Since the interface is impermeable to the gas, the diffusive flux of gas towards the liquid surface is exactly equal to the convective flux of gas away from the liquid surface; i e , the net transport of gas at the surface of the liquid film is zero.[1] Thus

$$(\rho v_d)_{g,S} = - (\rho_g v)_S \tag{2-18}$$

Hence

$$v_{d,g,S} = - v_S \tag{2-19}$$

[1] Note, however, that the concentration of the gas is always greater than zero at the interface

Equations 2-17 and 2-19 can be combined to yield

$$(\rho v_d)_{v,S} = (1 - C_{v,S})(\rho v)_S \tag{2-20}$$

Equations 2-12 and 2-20 can be combined to yield

$$(\rho v)_S = (\rho v)_{v,S} \tag{2-21}$$

Hence, Eqs. 2-20 and 2-21 show that at the interface, the diffusive rate of vapor transport, $(\rho v_d)_{v,S}$, and the total rate of vapor transport, $(\rho v)_{v,S}$, are related by

$$(\rho v_d)_{v,S} = (1 - C_{v,S})(\rho v)_{v,S} \tag{2-22}$$

It follows from the conservation of the evaporating species across the interface and from Equations 2-21, 2-22, and 2-15, that

$$(\rho v)_{v,S} = (\rho v)_L = (\rho v)_S = - \left[\frac{\bar{\rho}(D+D_t)}{1-C_v} \frac{\partial C_v}{\partial y} \right]_S \tag{2-23}$$

Equations 2-15, 2-17, 2-19, 2-22, and 2-23 describe, for the process of evaporation, the pertinent relationships between the several mass fluxes presented in Fig 2-6 Those equations also can be written in terms of the partial pressure of the vapor Consider Eq 2-15: from the definitions of the concentration of the vapor, C_v, and the partial pressure of the vapor, p_v, it follows that

$$\frac{\partial C_v}{\partial y} = \frac{\partial}{\partial y} \left(\frac{p_v R}{p R_v} \right) = \frac{R}{p R_v} \frac{\partial p_v}{\partial y} + \frac{C_v}{R} \frac{\partial R}{\partial y} \tag{2-24}$$

The perfect gas constant for the gas-vapor mixture can be written as

$$R = C_v R_v + (1-C_v) R_g \tag{2-25}$$

Hence

$$\frac{\partial R}{\partial y} = (R_v - R_g) \frac{\partial C_v}{\partial y} \tag{2-26}$$

Substituting Eq. 2-26 into Eq. 2-24, solving for $\partial C_v/\partial y$; and utilizing Eq. 2-25 yields

$$\frac{\partial C_v}{\partial y} = \frac{R^2}{R_v R_g} \frac{1}{p} \frac{\partial p_v}{\partial y} \tag{2.27a}$$

$$= \frac{1-C_v}{p-p_v} \frac{R}{R_v} \frac{\partial p_v}{\partial y} \tag{2.27b}$$

Substituting Eq. 2-27a into Eq. 2-15 yields the following expression for the diffusive rate of vapor transport at any station y:

$$(\rho v_d)_v = - \rho (D+D_t) \frac{R^2}{R_g R_v} \frac{1}{p} \frac{\partial p_v}{\partial y} \tag{2-28}$$

Equations 2-27b and 2-23 can be combined to yield the following expression for the conservation of mass across the interface:

$$(\rho v)_S = (\rho v)_L = (\rho v)_{v,S} = - \left| \frac{\bar{\rho}(D+D_t) R}{R_v (p-p_v)} \frac{\partial p_v}{\partial y} \right|_S \tag{2-29}$$

2.2.2 Interfacial Energy Balance

Figure 2-7 illustrates a general energy-transfer interface element placed at the surface of a stable, non-reactive liquid film. The different energy fluxes involved are defined as follows:

(1) $q_S = (k \frac{\partial t}{\partial y})_S$ = the rate at which energy is transferred across the S-surface by conduction

(2) $q_L = (k \frac{\partial t}{\partial y})_L$ = the rate at which energy is transferred across the L-surface by conduction.

(3) $(\rho v)_{v,S} h_{v,S}$ = the rate at which energy is convected across the S-surface by the evaporated vapor.

(4) $(\rho v)_L h_L$ = the rate at which energy is convected across the L-surface by the evaporating liquid.

(5) $q_{r,S}$ = the rate at which energy is transferred across the S-surface by radiation

(6) $q_{r,L}$ = the rate at which energy is transferred across the L-surface by radiation

(7) $(KE)_S \quad (\rho v)_S \quad (\frac{u_S^2}{2} + \frac{v_S^2}{2})$ = the rate at which kinetic energy associated with the gas-vapor phase crosses the S-surface.

(8) $(KE)_L \quad (\rho v)_L \quad (\frac{u_L^2}{2} + \frac{v_L^2}{2})$ = the rate at which kinetic energy associated with the liquid phase crosses the L-surface.

Since the net transport of the gas at the surface of the liquid film is zero,[1] only the transport of enthalpy associated with the evaporated vapor (see Item (3) above) needs be considered on the gas-vapor side of the interface. It is desirable, therefore, that

[1] See discussion leading to Eq 2-18.

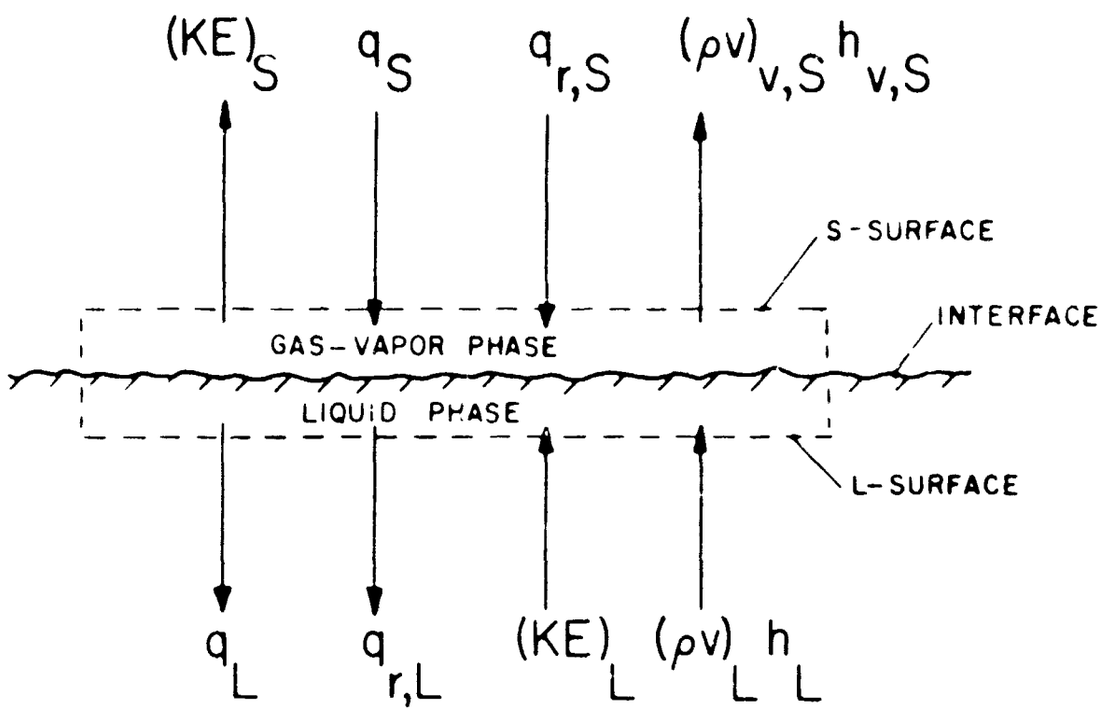

FIG. 2-7. AN ENERGY-TRANSFER INTERFACE ELEMENT FOR A STABLE, NON-REACTIVE LIQUID FILM

the vapor have a relatively large specific heat so that the vapor will cause a large amount of thermal "blockage."

In view of Eq. 2-23, the energy balance for the interface element illustrated in Fig. 2-7 can be written as follows:

$$\underset{I}{q_S} = \underset{II}{q_L} + \underset{III}{\left|\overline{(KE)}_S - \overline{(KE)}_L\right|} + \underset{IV}{(\rho v)_S(h_{v,S}-h_L)} - \underset{V}{(q_{r,S}-q_{r,L})} \qquad (2\text{-}30)$$

Term IV in Eq. 2-30 can be rewritten in the form

$$(\rho v)_S \, \Delta H_v$$

where ΔH_v is the latent heat of vaporization for the liquid coolant which corresponds to the saturation conditions prescribed by the partial pressure of the vapor at the interface. If the partial pressure of the vapor at the interface is equal to or greater than the critical pressure for the liquid coolant, then term IV in Eq 2-30 is identically zero. In most instances, term III in Eq. 2-30 can be considered negligible in comparison to a term such as term I Thus, neglecting term III, Eq. 2-30 can be rewritten to yield

$$q_L + q_{r,L} = q_S + q_{r,S} - (\rho v)_S \, \Delta H_v \qquad (2\text{-}31)$$

Equation 2-31 is the general energy balance for conditions at the interface. To obtain a better understanding of what is involved in evaluating the left-hand side of Eq. 2-31, the energy balance for the entire liquid film must be considered, and that energy balance is developed in the following section.

2.3 Energy Balance on the Liquid Film

2.3.1 General Energy Balance

Figure 2-8 illustrates diagrammatically a control volume placed within a stable, non-reactive liquid film. The following energy fluxes may be defined:

(1) $m'_o h_{l,o}$ = the rate of enthalpy transfer into the control volume per unit spanwise length due to the continuous injection of film coolant.

(2) $q_w \equiv (k \frac{\partial t}{\partial y})_w$ = the rate of conduction of heat from the liquid film to the wall.

(3) $q_{r,w}$ = the rate of radiant energy transfer to the wall.

The rate of injection of liquid into the control volume illustrated in Fig. 2-8 per unit spanwise length is denoted by m'_o. From the conservation of liquid film coolant it follows that

$$m'_o = \int_{x_o}^{x_1} (\rho v)_S \, dx \tag{2-32}$$

Employing Eq. 2-32, the energy balance for the control volume presented in Fig. 2-8 is given by

$$\int_{x_o}^{x_1} (q_L + q_{r,L}) \, dx \qquad \int_{x_o}^{x_1} [(\rho v)_S (h_L - h_{l,o}) + q_w + q_{r,w}] dx \tag{2-33}$$

Equation 2-33 is the general energy balance for the liquid film. For the special case where the summation of the terms under

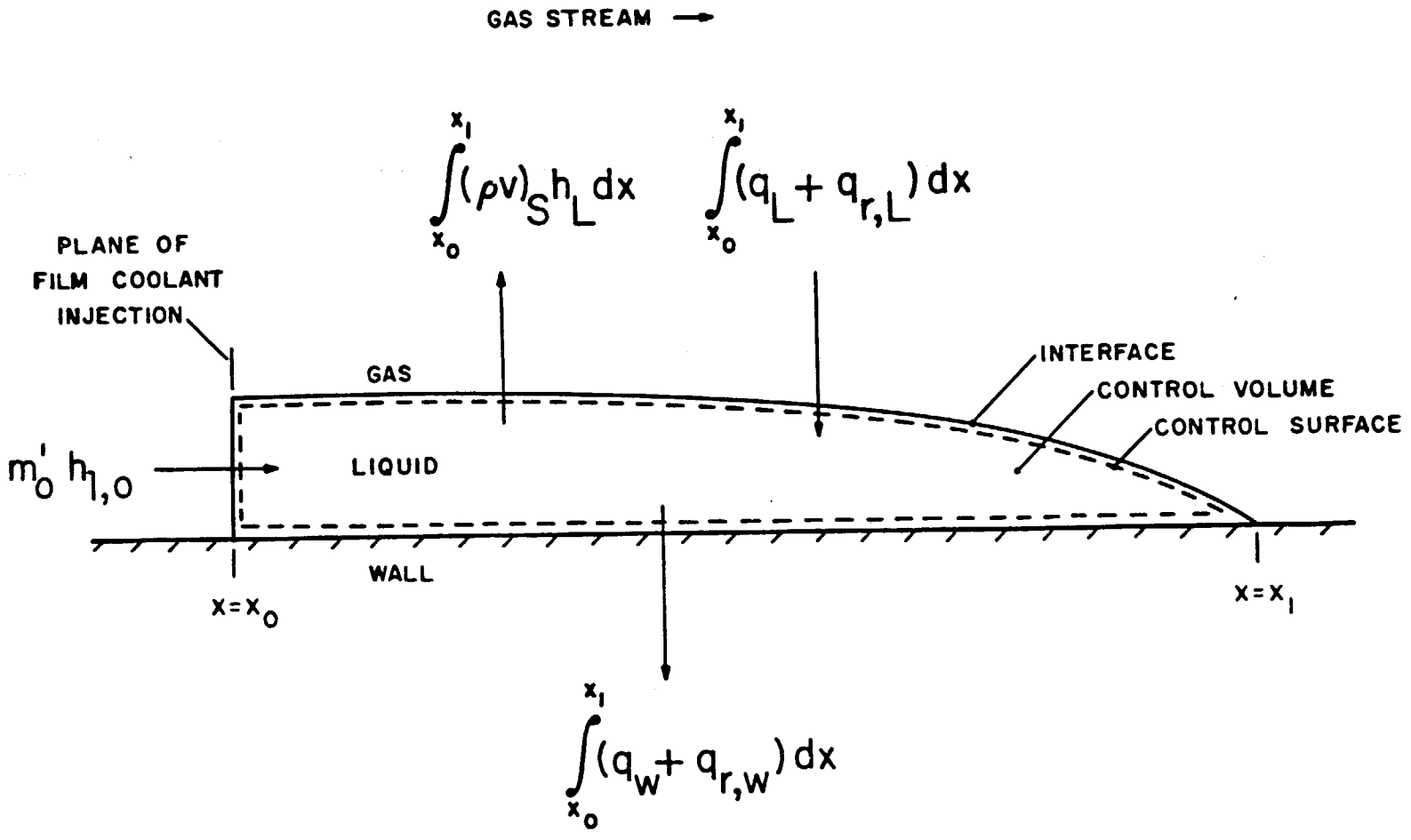

FIG. 2-8. CONTROL VOLUME FOR ENERGY BALANCE ON A STABLE, NON-REACTIVE LIQUID FILM

each of the integral signs in Eq. 2-33 is independent of x, the integral signs can be removed and one obtains a local energy balance for the liquid film. Furthermore, the relationship obtained after removing the integral signs can be combined with Eq. 2-31, obtaining thereby a local energy balance at the interface. Thus

$$q_S + q_{r,S} = q_w + q_{r,w} + (\rho v)_S (h_L - h_{l,o}) + (\rho v)_S \Delta H_v \qquad (2\text{-}34)$$

In many liquid-film cooling applications of interest, however, the terms under the integral signs in Eq. 2-33 are not independent of the streamwise coordinate x. Of particular interest is the problem of liquid-film cooling an exhaust nozzle wherein severe pressure gradients are common, and wherein the various terms in Eq. 2-33 are most certainly functions of x. In such a situation it is difficult to appraise the error involved when it is assumed that Eq. 2-34 is the local energy balance at the interface. In particular, it is difficult to appraise the error due to assuming that the portion of the incident heat flux utilized for increasing the sensible enthalpy of the liquid is equal to $(\rho v)_S (h_L - h_{l,o})$, as given by Eq. 2-34. Since Eq. 2-34 is much more convenient to employ, however, than is Eq. 2-31, further consideration of the problem is worthwhile. A method for experimentally investigating that problem is suggested in Section 3.3.1.

2 3.2 Simplified Energy Balances Employed by Previous Investigators

Knuth (8) simplified the general interfacial energy balance (see Eq 2-31) by assuming, in essence, that

$$q_{r,S} = q_L + q_{r,L}$$

In other words, Knuth equated the radiant energy incident on the surface of the liquid film to the energy utilized for increasing the sensible enthalpy of the liquid coolant plus the energy transferred to the solid surface wetted by the film. (In Knuth's experimental investigation, the wetted surface was approximately adiabatic.) Knuth, therefore, employed the following interfacial energy balance Thus

$$q_S = (\rho v)_S \Delta H_v \qquad (2\text{-}35)$$

Crocco (9) utilized the same interfacial energy balance as Knuth, but Crocco's reasoning was somewhat different. He assumed that the rate of radiant energy transfer to the liquid film was negligible and that the wetted surface was adiabatic Crocco further assumed that in a so-called "first period of existence," all of the film coolant was heated to equilibrium saturation conditions, and that for the major portion of the liquid-flow regime, all of the energy incident on the liquid film was utilized for evaporating it. Moreover, the analysis was concerned only with that major portion of the liquid-flow regime

Graham (10), Sellers (11), Kinney (5), and Emmons (6) employed an interfacial energy balance which is a simplification of Eq. 2-34. First, it was assumed that the radiant energy transfer was negligible. Furthermore, in the experimental investigations conducted by Graham, Kinney, and Sellers, and in a portion of the experimental investigation conducted by Emmons, the wetted surface was essentially adiabatic. Thus, the interfacial energy balance employed by those investigators for the case where the wetted surface was adiabatic is

$$q_S = (\rho v)_S (h_L - h_{l,o}) + (\rho v)_S \Delta H_v \qquad (2\text{-}36)$$

2.4 Gas-Liquid Interactions

The specification of the physical characteristics of the gas-liquid interface is of primary importance in the analysis of liquid-film cooling. Considerable experimental data are available that indicate that the interfacial structure has a considerable influence on the flow rate of film coolant required for establishing a specified liquid-film-cooled length (5)(8)(10)(11). Of particular significance is the phenomenon of film instability which causes the entrainment of liquid coolant droplets by the flowing gas stream. The physical nature of the gas-liquid interface is discussed in Section 2.4.1 and the phenomena of film instability and entrainment are discussed in Section 2.4.2.

2.4.1 Interfacial Structures

There appear to be three distinct interfacial structures associated with the process of liquid-film cooling that are of

interest. Figure 2-9 presents photographs of each of those interfacial structures. The photographs were taken during certain preliminary investigations conducted at the Jet Propulsion Center, Purdue University (12). The following features of the basic flow system and of the photographic apparatus are noteworthy: (a) the gaseous and liquid phases were air and deionized water, respectively; (b) the gaseous flow was turbulent; (c) a 35 mm camera equipped with a close-copy lens was employed in conjunction with a stroboscopic light source, which had a flash time of 2 microseconds, so that the gas side of the two-phase interface could be photographed; and (d) the optical line of sight was at an angle of 10^{o} with respect to the wetted test surface which was a highly polished, flat, stainless steel plate having a spanwise dimension of 4 ins..

The photographs presented in Fig. 2-9 were taken when the static pressure and the main-stream temperature had values of 220 psia and 1000 R, respectively. Flow parameters which were not common to all of the photographs are specified in the appropriate subtitles of Fig. 2-9; they are the main-stream velocity, u_e, the position downstream of the point of liquid-film coolant injection at which the photographs were taken, $x - x_0$, and the rate of liquid-film coolant injection per inch of injector slot width, m'_0.

The interfacial structure presented in Fig. 2-9a is characterized by its extreme smoothness. In that particular photograph there is shown a ½ in. diameter cylindrical plug which protrudes approximately 0.001 in. above the surface of the polished stainless steel surface.

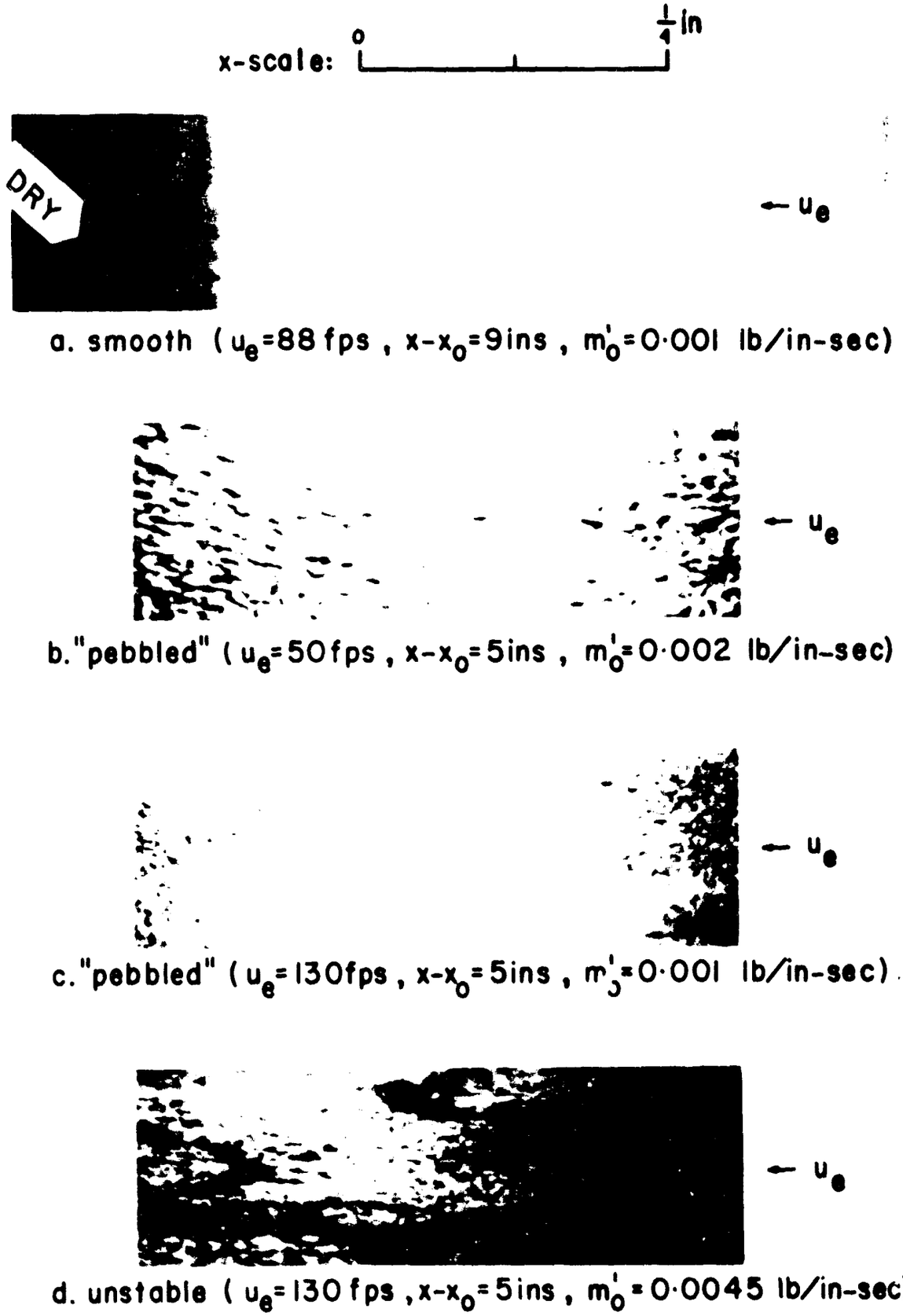

a. smooth (u_e=88 fps , $x-x_0$=9ins , m'_0=0·001 lb/in-sec)

b."pebbled" (u_e=50fps , $x-x_0$=5ins , m'_0=0·002 lb/in-sec)

c."pebbled" (u_e=130fps , $x-x_0$=5ins , m'_0=0·001 lb/in-sec)

d. unstable (u_e=130 fps , $x-x_0$=5ins , m'_0=0·0045 lb/in-sec)

FIG. 2-9. CHARACTERISTIC INTERFACIAL STRUCTURES FOR LIQUID-FILM COOLING

The fortuitous presence of that surface irregularity serves to indicate that a liquid film which has a smooth interfacial structure is, in general, very thin and sensitive to relatively small surface roughnesses. The smooth character of the interfacial structure is apparently due to the fact that the liquid film is so thin and viscous that any disturbances imparted to it as a consequence of turbulent velocity fluctuations in the adjacent gas phase are completely suppressed or "damped out." Because of the aforementioned sensitivity of a thin film to surface roughnesses, it is highly improbable that the liquid films employed for liquid-film cooling the walls of a rocket thrust chamber will have an extremely smooth interfacial structure.

The interfacial structure presented in Figs. 2-9b and 2-9c is quite common and is characterized by its "pebbled" appearance. The small disturbances which are evident on the surface of the liquid film are apparently a consequence of turbulent velocity fluctuations in the gas phase flowing past the liquid film (13). The liquid film is sufficiently thin and viscous that small disturbances which appear on its surface do not amplify and cause film instability. (It should not be implied, however, that there may not exist turbulent stresses in the liquid film.) The difference in the scale of the interfacial disturbances for the two "pebbled" interfaces presented in Fig. 2-9 is due primarily to a corresponding difference in the scale of the turbulence in the adjacent flowing gas; the turbulence scale of the gas phase decreases with increasing gas mass flow rate. That relationship between the gas mass flow rate and the nature of the "pebbled"

interfacial structure has been observed previously (5)(8)(13)(14).

The interfacial structure presented in Fig. 2-9d defines the phenomenon of film instability; the latter is characterized by the existence of large-scale disturbances which are turbulent in nature, and which are superimposed on a "pebbled" interfacial structure The phenomenon of film instability and the related phenomenon of liquid entrainment are discussed in the following section.

2.4.2 Film Instability and Entrainment

A large degree of liquid entrainment is known to occur when large-scale disturbances appear on the surface of a liquid film (15). Such entrainment reduces the effectiveness of the liquid-film cooling process in either or both of two ways:

1. If the entrained coolant is convected out of the region which is to be liquid-film cooled before it is evaporated, then a corresponding loss in liquid-film cooling effectiveness arises due to the incomplete utilization of the available heat of vaporization associated with the flow of the liquid-film coolant.
2. If the entrained liquid droplets are evaporated immediately upon leaving the interface, then the corresponding multi-fold increase in the specific volume of the coolant upon evaporation will have a disturbing effect on the gaseous boundary layer structure which, in turn, might tend to promote the degree of turbulent heat, mass, and momentum transport near the gas-liquid interface. Luikov (16, 17) has termed such a phenomenon volumetric boiling.

Thus, a problem of primary importance is that concerned with the specification of (a) the physical conditions under which small-scale interfacial disturbances will amplify and cause film instability, and (b) the degree of and the effects of liquid coolant entrainment once transition has occurred. Intuitively, parameters which may be of importance in a formulation of the solution to the above problem are as follows:

(i) the interfacial shear stress, τ_s, which represents the degree to which the gaseous flow regime tends to deform the liquid film;

(ii) the dynamic viscosity of the liquid, μ_l, which is a measure of the resistance of the liquid film to deformation;

(iii) the thickness of the liquid film, δ_f, which represents the extent to which the gas-liquid interface experiences the stabilizing influence of the wetted solid surface;

(iv) the kinematic viscosity of the liquid, ν_l, which is a measure of the damping characteristics of the liquid film;

(v) the interfacial density ratio, ρ_s/ρ_l, which represents the relative inertia characteristics of the two phases, and is a measure of the degree to which a turbulent velocity fluctuation in the gaseous phase will influence the liquid-flow regime;

(vi) the dynamic viscosity ratio μ_s/μ_l, which is a measure of the discontinuity in the velocity profile at the gas-liquid interface; and

(vii) the surface tension of the liquid phase.

References (5)(13)(14)(15) have experimentally investigated the phenomenon of film instability. Subsequent attempts to correlate the

inception of film instability have employed the dimensionless liquid-flow rate W^+ (see Eq. 2-10). It is of interest to note that W^+ combines the individual influences of the parameters (i)-(iv) listed above into a single parameter.

The motivation for attempting to correlate the inception of film instability in terms of the single parameter W^+ arises from the following facts which characterize single phase turbulent flow: (a) a universal relationship between u^+ and y^+ (the "law-of-the-wall") characterizes the "inner" region ($y^+ < 1000$) of the wall turbulent region[1]; and (b) the distance normal to the wall at which turbulent forces are of the same order of importance as the viscous forces is defined approximately by $15 < y^+ < 20$ and $90 < W^+ < 150$ (5)(18). Thus, the transition state for the liquid-flow regime would be characterized by corresponding limits of δ_f^+ and W^+ if the following basic hypothesis is physically correct: (1) parameters (v)-(vii), presented in the foregoing, do not appreciably affect the transition characteristics of the liquid-flow regime; (2) the liquid-flow regime obeys the universal "law-of-the-wall" as established for single phase flow; and (3) transition occurs when the turbulent forces in the region of the liquid film close to the gas-liquid interface are of the same order of importance as the viscous forces.

While a large percentage of the experimental data tends to substantiate the foregoing simple hypothesis (5)(15), a limited amount of data has been obtained which indicates that the simple hypothesis may not give a complete characterization of the phenomena.

[1] See Fig. 2-3.

For example, experimental observations indicate that the critical value of W^+ increases slightly with decreasing surface tension (5), and that the parameter μ_s/μ_l may also be significant in defining the transition state (13)(14). Furthermore, at relatively low values of the gas stream Reynolds number[1] ($<10^4$) it is known that the critical value of W^+ can increase significantly (19); i.e., the transition state is a function of both the Reynolds number for the gas stream and W^+. It would appear, however, that at values of the gas stream Reynolds number which are most commonly associated with the gas flow in a rocket thrust chamber ($>10^5$), the dependence of the critical value of W^+ on the Reynolds number for the gas stream is negligible (5)(14)(19).

For the practical design of a liquid-film-cooled system which is characterized by gas-stream Reynolds numbers greater than 10^5, the following generalized results given by Kinney, et al. (5) appear to be adequate until a more complete theory is formulated and substantially verified:

1. In the situation where the evaporation rate is negligible, and wherein m' is thus independent of the streamwise coordinate x, the inception of film instability is approximately defined by $W_o^+ = 90$ where

$$W_o^+ = \frac{m'_o}{\mu_l} \tag{2-37}$$

The viscosity μ_l in Eq. 2-37 is evaluated at a streamwise-mean liquid-film temperature.

---

[1] The Reynolds number referred to on this page is R_d, defined on page 57.

2. In the case of liquid-film cooling, wherein the value of W^+ varies from a nonzero value at $x = x_o$ to zero at $x = x_1$, the onset of a high degree of liquid entrainment--which accompanies a corresponding decrease in liquid-film cooling effectiveness--is approximately defined by $W_o^+ = 360$.

Graham (10,20) experimentally investigated the relationship between the effectiveness of liquid-film cooling and the phenomenon of liquid entrainment. He introduced a stability effectiveness ϵ_s defined by

$$\epsilon_s = \frac{m'_{o,i}}{m'_{o,a}} \tag{2-38}$$

where

$m'_{o,i}$ = the ideal rate of coolant consumption (zero entrainment).

$m'_{o,a}$ = the actual rate of coolant consumption.

Graham correlated ϵ_s in terms of W_o^+ utilizing the experimental data of References (5) and (10); the resultant correlation for smooth-tube flow is presented in Fig. 2-10. It should be noted that the correlation was developed utilizing the assumption that the heat transfer film coefficient h'_s is independent of W_o^+. There appear to exist, however, considerable experimental data which indicate that h'_s is significantly dependent on W_o^+; the latter phenomenon is discussed in Section 3.2.

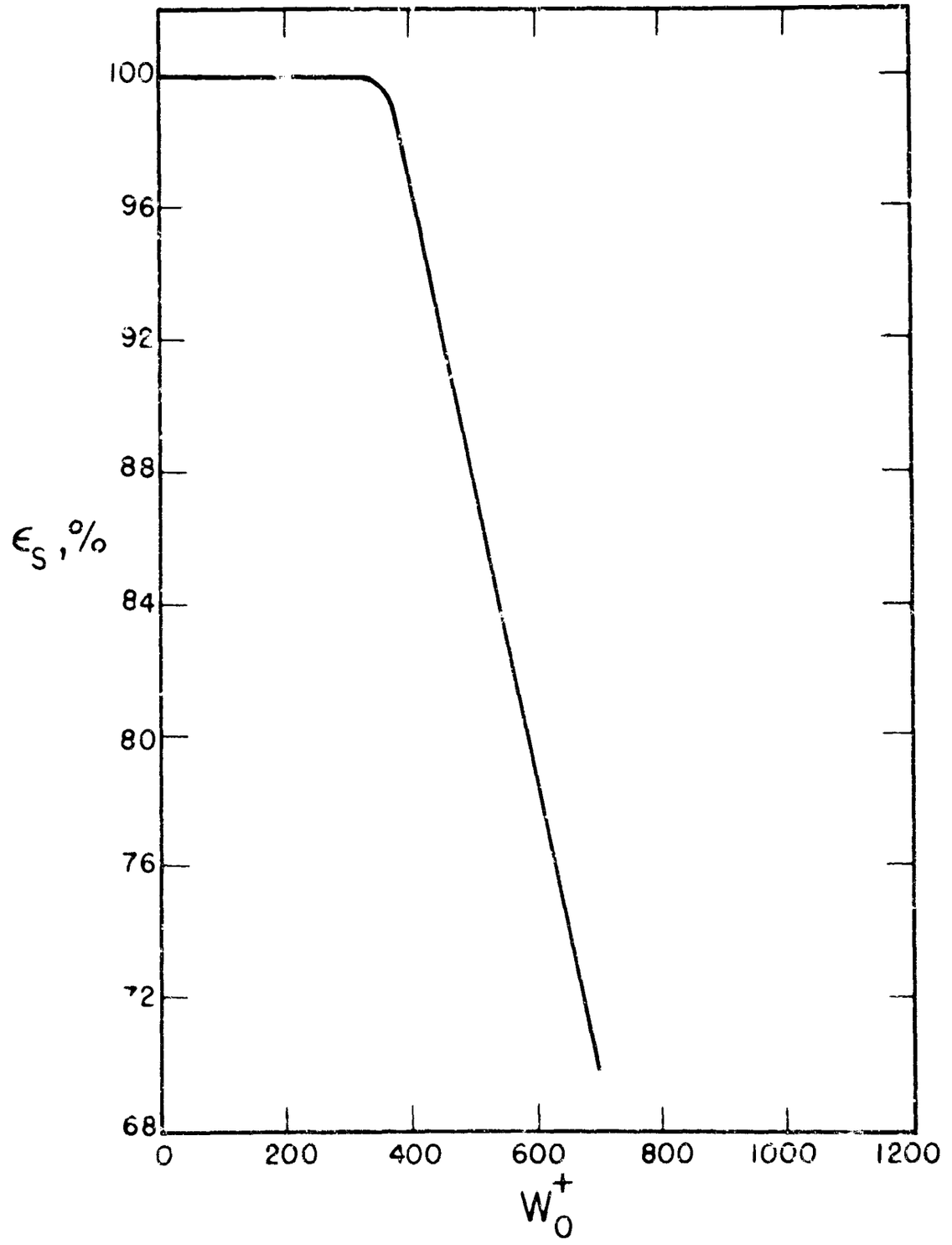

FIG. 2-10. THE CORRELATION DUE TO GRAHAM(10) FOR THE STABILITY EFFECTIVENESS ϵ_s AS A FUNCTION OF THE LIQUID FLOW RATE PARAMETER W_0^+

The stability effectiveness ϵ_s represents a measure of an effect of the entrainment phenomenon rather than a direct measure of the actual quantity of coolant which is entrained by a flowing gas stream. The latter problem has been experimentally investigated by Hewitt, et al. (21) for the case of annular two phase flow. In that subject investigation the quantity of entrained liquid was determined by employing a sampling probe which traversed the central core of the two-phase flow field. It was observed that below a critical value of liquid flow rate, the entrainment was negligible; the critical state was approximately defined by $W_o^+ = 90$ (15). As the liquid flow rate increased above the critical value, the trainment of liquid into the central gas core increased correspondingly. It was observed, however, that the degree of entrainment increased with increasing rate of gas flow as well as with increasing rate of liquid flow. Furthermore, additional experiments conducted at different system pressures indicated that the degree of entrainment increased with decreased pressure, the mass flow rate of gas being held constant. Those two facts would indicate that the interfacial shear stress τ_s, in addition to the dimensionless liquid flow rate W_o^+, might be of significance in determining the actual quantity of coolant which is entrained by a flowing gas stream.

The values of the experimental parameters investigated by Hewitt, et al. (21) were significantly different from those which would normally characterize an application of liquid-film cooling. In particular, the temperature and pressure employed were essentially ambient and the evaporative rate of mass transfer was zero. It is

impossible, therefore, to determine from those data the relationship which exists between the stability effectiveness ϵ_s and the actual quantity of coolant which is entrained by a flowing gas stream. It would appear that a need exists for additional experimental investigation of the phenomenon of liquid entrainment.

3. ANALYZING THE LIQUID-FILM-COOLED REGION

A review of the previous analyses for liquid-film cooling is presented in Section 3.1, and a review of some pertinent experimental data is presented in Section 3 2. The latter serves to illustrate the limitations of those analyses that are reviewed, and provides the motivation for the alternate correlation procedure that is presented in Section 3.3 for heat-mass transfer data that are obtained in liquid-film cooling experiments

3.1 A Review of the Previous Analyses

Table 1 compares the analyses due to Knuth (8), Sellers (11)(22), Graham (10), Rannie (23)[1], and Emmons (6). Column I of that table shows that similar sets of equations are employed in the analyses due to Knuth, Sellers, Graham, and Rannie; consequently, those analyses are considered concurrently in Section 3.1 1. Because the analysis due to Emmons is the most recent analysis developed, and also since it differs fundamentally from the earlier analyses, that analysis is considered separately in Section 3 1 2

The fundamental steps that are common to each of the subject analyses are outlined briefly below:

Step 1. Elementary boundary-layer theory is employed to analyze the gaseous-flow regime above the liquid film. In the analyses due to Knuth,

[1] As modified for liquid-film cooling by Sloop (24).

TABLE I

A COMPARISON OF THE PREVIOUS ANALYSE

COLUMN →	I	II	III
REFERENCE	EQUATIONS EMPLOYED	UNKNOWNS ELIMINATED FROM EQUATIONS EMPLOYED	THE FUNDAMENTAL ANALYTICAL SOLUTION(S) FOR $\beta \equiv$
RANNIE (23)	3-4*, 3-5*, 3-6, 3-7, and terms (b) and (c) of 3-10	τ_δ, τ_s, t_δ, q_δ	$\beta + 1 = \left[1 + \frac{C_{p_v}}{C_p}\left(\frac{u_e}{u_\delta} - 1\right)\left\{1 - \exp\left(-\frac{(\rho v)_s}{\mu}\delta\right)\right\}\right] \exp($
SELLERS (22)		τ_δ, t_δ, q_δ, δ	$\beta + 1 = \left[1 + \frac{\frac{(\rho v)_s}{(\rho u)_e}}{\left(\frac{u_e}{u_\delta}\right)\left(\frac{\tau_s}{\rho_e u_e^2}\right)}\right]^{\frac{C_{p_v}}{C_p} Pr} \times \left[1 + \frac{\frac{C_{p_v}}{C_p}\left(\frac{u}{}\right.}{1 + \left(\frac{\tau_s}{\rho_e u_e^2}\right)}\right.$
SELLERS (11)	3-6, 3-7, terms (b) and (c) of 3-10 and terms (a) and (c) of 3-14	$\frac{\tau_\delta}{q_\delta}$, t_δ, δ	$\beta + 1 = \left[1 + \frac{\frac{(\rho v)_s}{(\rho u)_e}}{\left(\frac{u_e}{u_\delta}\right)\left(\frac{\tau_s}{\rho_e u_e^2}\right)}\right]^{\frac{C_{p_v}}{C_p} Pr} \times \left[\frac{1}{Pr}\left(\frac{u_e}{u_\delta} - 1\right) + 1\right]$
SELLERS (11,22)	3-6, 3-7, terms (b) and (c) of 3-10, and terms (b) and (c) of 3-14	$\frac{\tau_\delta}{q_\delta}$, t_δ, δ	$\beta + 1 = \left[1 + \frac{\frac{(\rho v)_s}{(\rho u)_e}}{\left(\frac{u_e}{u_\delta}\right)\left(\frac{\tau_s}{\rho_e u_e^2}\right)}\right]^{\frac{C_{p_v}}{C_p} Pr} + \left[\frac{\frac{(\rho v)_s}{(\rho u)_e}}{\left(\frac{u_e}{u_\delta}\right)\left(\frac{\tau_s}{\rho_e u_e^2}\right)}\right] \left(\frac{C_{p}}{C_{p}}\right.$
GRAHAM (10)			(Graham assumed $(C_{p_v}/C_p)Pr = 1$)
KNUTH (8)	3-3*, 3-4*, 3-5*, 3-6, 3-7, 3-8, 3-12, and data for $p_{v,s} = f(t_s)$	τ_s, t_δ, u_δ, $p_{v,\delta}$, q_δ, $(\rho v)_\delta$	$\beta + 1 = \left[1 + \frac{(\rho v)_s}{\tau_\delta} u_e \exp\left(\frac{(\rho v)_s}{\mu}\delta\right)\right]^{\frac{C_{p_v}}{C_p}} \exp\left(\frac{C_{p_v}}{C_p}\right.$
			$\beta + 1 = \left[\frac{p - p_{v,e}}{p - p_{v,s}}\right]^{\frac{C_{p_v}}{C_p}\frac{R}{R_v}} \exp\left(\frac{C_{p_v}}{C_p}(Pr - Sc)\frac{(\rho v)_s}{\mu}\right.$
EMMONS (6)	3-17 and 3-18	τ_s	Equation due to Emmons* $\beta = \frac{C_{p_v}}{C_p}\frac{(\rho v)_s}{(\rho u)_e}\left(\frac{\rho_e u_e^2}{\tau_{s,0}}\right) \exp\left[\frac{13.89}{b} - \frac{v_s}{(\tau_{s,0}/\rho)^{1/2}}\right.$
			As corrected by writer $\beta = \frac{C_{p_v}}{C_p}\frac{(\rho v)_s}{(\rho u)_e}\left(\frac{\rho_e u_e^2}{\tau_{s,0}}\right) \exp\left\{\frac{13.89}{b}\frac{v_s}{u_e}\left[\frac{1}{\beta}\right.\right.$

*Evaluated at $y = \delta$

*Eq B-19 of Ref (6)

E I

YSES FOR LIQUID-FILM COOLING

	IV	V
$\beta \equiv \frac{(\rho v)_S \, C_{p_v} (t_e - t_s)}{q_S}$	EMPIRICAL AND/OR EXPERIMENTAL EVALUATION OF THE REMAINING UNKNOWNS	THE INTERFACIAL ENERGY BALANCE EMPLOYED
$\exp\left(Pr \frac{C_{p_v}}{C_p} \frac{(\rho v)_S}{\mu} \delta\right)$	1. $t_s = t_{sat}$ 2. $\delta = 5.6 \nu / (\tau_{s,o}/\rho)^{1/2}$ 3. $u_\delta = 5.6 (\tau_{s,o}/\rho)^{1/2}$	$\beta = \frac{C_{p_v}(t_e - t_s)}{(h_L - h_{l,o}) + \Delta H_v}$ *
$\frac{C_{p_v}}{\quad} \frac{u_e}{u_\delta} - 1)$ $\frac{\tau_s}{\quad} \frac{u_e}{u_\delta} \frac{(\rho u)_e}{(\rho v)_S}$	1. $t_s = t_{sat}$ 2. u_δ and τ_s were determined from the data of Ref. 5; the results were $\frac{u_e}{u_\delta} = 4.5$ $\frac{u_e}{u_\delta} \frac{\tau_s}{\rho_e u_e^2} = 0.00933$	
$+ 1\Big] - \frac{1}{Pr} \left(\frac{u_e}{u_\delta} - 1\right)$		$\beta = \frac{C_{p_v}(t_e - t_s)}{(h_L - h_{l,o}) + \Delta H_v}$
$\Big] \left(\frac{C_{p_v}}{C_p}\right)\left(\frac{u_e}{u_\delta} - 1\right)$	1. $t_s = t_{sat}$ 2. $u_\delta = 5.0 (\tau_s/\rho)^{1/2}$ 3. τ_s was determined from the data of Ref. 10	
$\frac{C_{p_v}}{C_p}(Pr - 1) \frac{(\rho v)_S}{\mu} \delta)$ $\frac{v)_S}{\quad} \delta)$	1. $\tau_\delta = \tau_{s,o}$ 2. $\delta = 5.6 \nu / (\tau_{s,o}/\rho)^{1/2}$ 3. $p_{v,s}$ and t_s were evaluated by simultaneously satisfying both of the equations given in column III for β and the thermodynamic data for $p_{v,s}$ as a function of t_s	$\beta = \frac{C_{p_v}(t_e - t_s)}{\Delta H_v}$
$\frac{\quad}{\rho)^{1/2}}\Big]$ $\frac{(\rho v)_S}{(\rho u)_e} \frac{C_{p_v}}{C_p} \frac{\rho_e}{\rho}\Big]^{-1/2}\Big\}$	1. $t_s = t_{sat}$ 2. b was determined from the data of Ref 6; the result was $b = 0.110$	$\beta = \frac{C_{p_v}(t_e - t_s)}{(h_L - h_{l,o}) + \Delta H_v}$

*Modification by Sloop (24)

*Modification by Sloop (24)

Rannie, Sellers, and Graham, the Prandtl-Taylor theory (18) is extended to include the effects of mass transfer. In the analysis due to Emmons, the theory developed by Turcotte (25) for the case of the transpired turbulent boundary layer on a flat plate is extended to the case of liquid-film cooling The result of those developments is basically an analytical expression for the following non-dimensional parameter[1,2]. Thus

$$\beta \quad \frac{(\rho v)_S \, c_{p_v} \, (t_e - t_s)}{q_S} \qquad (3\text{-}1)$$

where

q_S = the rate at which energy is transferred across the S-surface[3] by conduction.

$(\rho v)_c$ = the rate at which mass is transferred across the S-surface by convection

t_e = the temperature at the edge of the boundary layer, or on the axis of the duct.

t_s = the temperature at the gas-liquid interface.

c_{p_v} = the specific heat for the vapor.

Step 2. Another expression is developed for the parameter β by considering the conservation of energy across the gas-liquid interface[4]

---

[1] The parameter β was denoted by H in the original analyses due to Sellers, and is related to the Stanton number for heat transfer, defined by Eq 3-25

[2] See Table 1, column III

[3] See Section 2 2 1 for the definition of the S-surface.

[4] See Table 1, column V

That expression for β combined with the expression for β obtained in Step 1 yields, in principle, a single equation in the single unknown $(\rho v)_S$.

Step 3. Finally, from the conservation of mass for the liquid-film coolant, the coolant flow rate m'_0 is related to the liquid-film-cooled length L by

$$m'_0 = (\rho v)_S \, L \qquad (3\text{-}2)^1$$

Equation 3-2, which relates m'_0 and L, is what is desired as the result of each analysis.

In completing Step 1, which constitutes the major part of each analysis, there arises more unknown quantities than there are independent equations. To circumvent that difficulty, one of the following methods is employed:[2]

(a) Empirical formulae, based on zero mass transfer, are employed to obtain approximate values for the unknown quantities needed for completing the solution. The appropriateness of the assumptions employed is determined by comparing the analytical predictions with experimental data (8) (23).

(b) Some of the unknown quantities needed for completing the solution are approximated by means of empirical formulae, and the remainder are determined experimentally. An obvious disadvantage of the latter method

---

[1] Equation 3-2 follows from Eq. 2-32 and Assumption (1.f) of the analytical model that is presented in the following section.

[2] See Table 1, column IV.

is that the final analytical expression cannot be applied with confidence to situations that differ significantly from that for which the unknowns were determined. Sellers determined two unknowns and Graham and Emmons each determined one unknown from experimental data.

3.1.1 The Analyses Due to Rannie, Sellers, Graham, and Knuth

Discussed in the present section are the fundamental developments that relate to the completion of Step 1 for the subject analyses.

The Physical and Analytical Models. Figure 3-1 illustrates schematically a physical model characteristic of those employed by References (8)(11)(22)(10)(23). The assumptions common to the different analytical models are as follows:

(1)[1] The partial derivatives of the following parameters with respect to the streamwise coordinate x are zero:

(1.a) the streamwise component of velocity, u;

(1.b) the static temperature of the gas stream, t;

(1.c) the partial pressure of the vapor, p_v;

(1.d) the interfacial shear stress, τ_s;

(1.e) the rate at which heat is transferred across the S-surface by conduction, q_s; and

(1.f) the rate at which mass is transferred across the S-surface by convection $(\rho v)_s$.

(2) The gaseous flow regime is subdivided into an "effective" laminar sublayer, bounded by $y = 0$ and $y = \delta$, and a turbulent core, bounded by $y = \delta$ and $y = \Delta$.

[1] Assumption (1) is equivalent to either the assumption of fully-developed-pipe flow or the assumption of Couette flow.

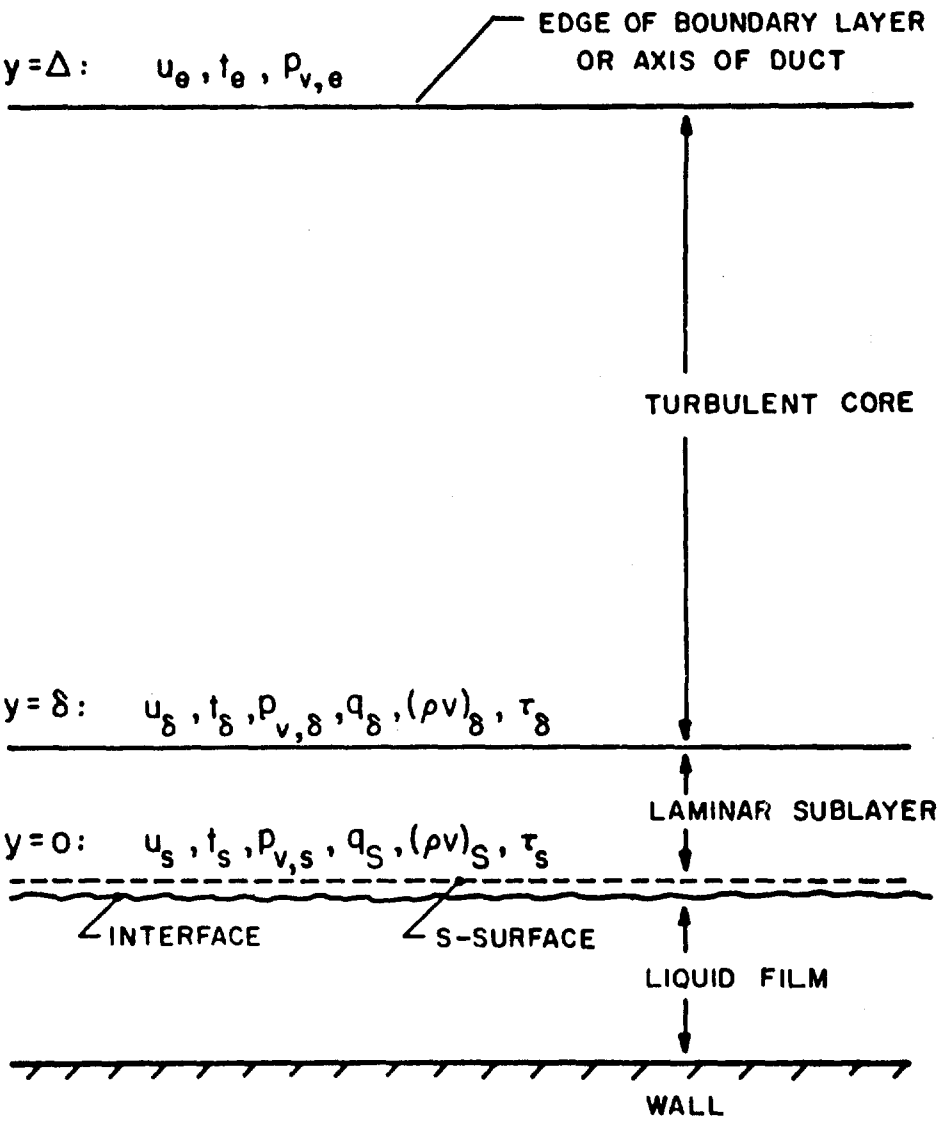

FIG. 3-1. A SCHEMATIC REPRESENTATION OF THE PHYSICAL MODEL EMPLOYED IN THE SUBJECT ANALYSES

(3) The wetted surface is adiabatic.

(4) The liquid-film coolant is non-reactive, and the interfacial surface is stable.

(5) The flowing gas is incompressible, and its properties may be evaluated at a suitable reference temperature.

(6) The effects of mass transfer upon heat transfer and momentum transfer are important only in the laminar sublayer (except in Knuth's analysis where said effects are also considered in the turbulent core).

(7) The turbulent Prandtl number and Schmidt number, defined by $Pr_t \equiv \frac{\mu_t}{k_t} c_p$ and $Sc_t \equiv \frac{\mu_t}{\rho D_t}$, respectively, are unity.

(8) The surface velocity of the liquid film is negligible compared to the main-stream velocity u_e.

(9) Across the "thin" laminar sublayer it can be assumed that

$$(9.a) \quad (\rho v) = \frac{-DR\rho}{R_v(p-p_v)} \frac{dp_v}{dy} = \text{constant} = (\rho v)_s \qquad (3\text{-}3)$$

$$(9.b) \quad \mu \frac{du}{dy} - (\rho v)_s u = \text{constant} = \tau_s \qquad (3\text{-}4)$$

$$(9.c) \quad k \frac{dt}{dy} - (\rho v)_s c_{p_v} t = \text{constant} = q_s - (\rho v)_s c_{p_v} t_s \qquad (3\text{-}5)^1$$

---

[1] It is argued in Ref. (26), pp. 10-12, that the specific heat for the vapor in Eq. 3-5 should be replaced by the specific heat for the gas-vapor mixture. However, that argument is incorrect due to the fact that the diffusive mode of mass transport was not considered (see the developments leading to Eqs. 2-18 and 2-30).

The Resistance of the Laminar Sublayer to Momentum Transfer. It follows that by integrating Eq. 3-4 and substituting the limits $u = 0$ at $y = 0$ and $u = u_\delta$ at $y = \delta$, one obtains an equation for the resistance of the laminar sublayer to momentum transfer. In dimensionless form, that equation is

$$\frac{u_\delta}{u_e} = \frac{\tau_s}{\rho_e u_e^2} \frac{(\rho u)_e}{(\rho v)_s} \left\{\exp\left(\frac{(\rho v)_s \delta}{\mu}\right) - 1\right\} \tag{3-6}$$

The Resistance of the Laminar Sublayer to Heat Transfer. It follows that by integrating Eq. 3-5 and introducing the limits $t = t_s$ at $y = 0$ and $t = t_\delta$ at $y = \delta$, one obtains an equation for the resistance of the laminar sublayer to heat transfer. In non-dimensional form that equation is

$$\frac{t_\delta - t_s}{t_e - t_s} = \frac{1}{\beta} \left\{\exp\left(Pr \frac{c_{p_v}}{c_p} \frac{(\rho v)_s}{\mu} \delta\right) - 1\right\} \tag{3-7}$$

The Resistance of the Laminar Sublayer to Mass Transfer. Of the subject analyses, only that analysis due to Knuth includes a specification of the vapor-partial-pressure field (or its equivalent, the vapor-concentration field). In general, the specification of that field may be desirable for one or more of the following reasons: (a) the evaluation of the physical and transport properties; (b) the evaluation of the energy released by chemical reactions in the case where the liquid-film coolant is reactive; and (c) the determination of the

temperature at the gas-liquid interface--which is uniquely related to the partial pressure of the vapor at the interface. If that temperature must be known with a high degree of accuracy, the approximation[1] introduced by Graham, Sellers, and Emmons is inappropriate. Knuth considered the problem of specifying the partial-pressure field for the latter reason.

For completeness, the specification of the partial pressure distribution is considered herein. Integrating Eq. 3-3 and imposing the limits $p_v = p_{v,s}$ at $y = 0$ and $p_v = p_{v,\delta}$ at $y = \delta$, the equation is obtained for the resistance of the laminar sublayer to mass transport, which in non-dimensional form is given by

$$\frac{p - p_{v,\delta}}{p - p_{v,s}} = \exp\left(Sc \frac{R_v}{R} \frac{(\rho v)_s}{\mu} \delta\right) \tag{3-8}$$

The Relative Resistance of the Turbulent Core to Mass, Momentum, and Heat Transfer (the Reynolds Analogy). A logical extension of the Reynolds analogy (18)(27) to heat, mass, and momentum transfer in the turbulent core of the gaseous-flow regime is

$$\frac{(\text{mass flux})_{y=y}}{(\text{mass flux})_{y=\delta}} = \frac{(\text{momentum flux})_{y=y}}{(\text{momentum flux})_{y=\delta}} = \frac{(\text{heat flux})_{y=y}}{(\text{heat flux})_{y=\delta}}$$

The above relationship can be written more explicitly in two ways: (a) based on the diffusive rates of transport only, and (b) based on the total rates of transport (diffusion plus convection). Rannie, Sellers, and Graham employed method (a); Knuth employed method (b).

[1] The approximation being that the temperature of the liquid film equals the saturation temperature of the film coolant which corresponds to the static pressure p.

The Reynolds analogy which considers only the diffusive mode of transport can be written as follows. Thus

$$\frac{-D_t \frac{\rho R}{R_v (p - p_v)} \frac{dp_v}{dy}}{(\rho v)_\delta} = \frac{\mu_t \frac{du}{dy}}{\tau_\delta} = \frac{k_t \frac{dt}{dy}}{q_\delta} \qquad (3\text{-}9)$$

where

q_δ = the rate at which energy is transferred across the surface $y = \delta$ by conduction.

$(\rho v)_\delta$ = the rate at which mass is transferred across the surface $y = \delta$ by convection.

τ_δ = the shear stress at $y = \delta$.

Integrating Eq 3-9, substituting the appropriate limits at $y = \delta$ and at $y = \Delta$, and introducing Assumption (7), yields

$$\frac{R}{R_v} \ln \left(\frac{p - p_{v,e}}{p - p_{v,\delta}}\right) = \frac{(\rho v)_\delta}{\tau_\delta} (u_e - u_\delta) = \frac{(\rho v)_\delta}{q_\delta} (t_e - t_\delta) c_p \qquad (3\text{-}10)$$

(a) (b) (c)

The Reynolds analogy that considers both convective and diffusive rates of transport can be written in the following form (8):

$$\frac{\frac{-D_t \rho R}{R_v (p-p_v)} \frac{dp_v}{dy}}{(\rho v)_\delta} = \frac{\mu_t \frac{du}{dy} + \frac{D_t R \rho}{R_v (p - p_v)} \frac{dp_v}{dy} u}{\tau_\delta - (\rho v)_\delta u_\delta} = \frac{k_t \frac{dt}{dy} + \frac{D_t \rho R}{R_v (p - p_v)} \frac{dp_v}{dy} c_{p_v} t}{q_\delta - (\rho v)_\delta c_{p_v} t_\delta} \qquad (3\text{-}11)$$

Integrating Eq. 3-11, substituting the appropriate limits at $y = \delta$ and at $y = \Delta$, and employing Assumption (7), one obtains (8)

$$\frac{R}{R_v} \ln \left(\frac{p - p_{v,e}}{p - p_{v,\delta}}\right) = \ln \left\{1 + \frac{(\rho v)_\delta}{\tau_\delta} (u_e - u_\delta) \right\}$$

$$= \frac{c_p}{c_{p_v}} \ln \left\{1 + \frac{(\rho v)_\delta}{q_\delta} (t_e - t_\delta) c_{p_v} \right\} \qquad (3\text{-}12)$$

Equations 3-10 and 3-12 are the two ways in which the Reynolds analogy can be employed to describe the relative resistance of the turbulent core to the transfer of heat, mass, and momentum. It should be noted that Assumption (9) (see page 47), which was employed to derive the equations for the laminar sublayer, is a special case of the Reynolds analogy that considers both diffusive and convective transport (Eq. 3-11). To consider two of the analyses due to Sellers, the Reynolds analogy that considers only diffusive heat and momentum transport must also be written for the laminar sublayer; i.e.,

$$\frac{k \frac{dt}{dy}}{\mu \frac{du}{dy}} = \frac{c_p}{Pr} \frac{dt}{du} = \text{a constant across the laminar sublayer} = \frac{q_S}{\tau_S} = \frac{q_\delta}{\tau_\delta} \qquad (3\text{-}13)$$

Integrating Eq. 3-13 across the sublayer and substituting the appropriate limits, one obtains[1]

---

[1] Sellers states that Eq. 3-14 implies that the velocity and temperature profiles in the laminar sublayer are assumed to be linear (11, p. 20); however, since Eq. 3-13 needs not be so restricted, it would appear that qualifying statement by Sellers is unnecessary.

$$\frac{t_\delta - t_s}{u_\delta} = \frac{Pr}{c_p}\frac{q_s}{\tau_s} = \frac{Pr}{c_p}\frac{q_\delta}{\tau_\delta} \qquad (3\text{-}14)$$

(a) (b) (c)

Comparing the Analyses. Equations 3-3 through 3-8 plus Eqs. 3-10, 3-12, and 3-14 represent the relationships from which the analyses due to Rannie, Sellers, Graham, and Knuth have been developed Table 1, p. 42, indicates the specific equations that are employed in each of the subject analyses (column I), together with the unknowns that are eliminated between those equations (column II) and the resultant analytical expression for the parameter β (column III) Also presented in that table are the empirical formulae and/or experimental data that are employed in each of the subject analyses (column IV), and the interfacial heat balance that is employed (column V)

3 1 2 The Analysis Due to Emmons[1]

Physical and Analytical Models. The physical and analytical models presented in Section 3 1 1 are applicable to the analysis due to Emmons, with the exception of Assumptions (2) and (9). Assumption (2) should be rewritten as follows: The gaseous-flow regime is subdivided into a turbulent core and a viscous sublayer region wherein the following eddy-viscosity relationship proposed by Turcotte (25) applies:

$$\frac{\mu_t}{\mu} = \sinh^2\left(\frac{by^+}{13.89}\right) \quad (y^+ < \delta^+;\ \delta^+ = 25.4) \qquad (3\text{-}15)$$

---

[1] To improve the clarity, completeness, and correctness of the original analysis due to Emmons, the developments and the final solution presented herein differ from that originally presented by Emmons; however, the analytical and physical models are the same.

The parameter b in Eq. 3-15 must be determined experimentally.[1]

Assumption (9) should be modified slightly in accordance with the new definition of the sublayer region; i.e., the molecular thermal conductivity k and dynamic viscosity μ should be replaced by their "effective" values, denoted by $k + k_t$ and $\mu + \mu_t$, respectively.

An additional significant assumption employed by Emmons is that the molecular Prandtl number, defined by $Pr = \frac{\mu c_p}{k}$, is equal to unity.

τ_s Related to q_s (The Reynolds Analogy). To relate the interfacial shear stress τ_s to the heat flux q_s, Emmons assumed that the basic Reynolds analogy, written as follows, is valid for the entire gaseous-flow regime:

$$\frac{k + k_t}{\mu + \mu_t} \frac{\frac{dt}{dy}}{\frac{du}{dy}} = \frac{\frac{\mu}{Pr} + \frac{\mu_t}{Pr_t}}{\mu + \mu_t} c_p \frac{dt}{du} = c_p \frac{dt}{du} = \frac{q_s}{\tau_s} \qquad (3\text{-}16)$$

Integrating Eq. 3-16 and substituting the appropriate limits at $y = 0$ and at $y = \Delta$, one obtains

$$c_p \frac{t_e - t_s}{u_e} = \frac{q_s'}{\tau_s} \qquad (3\text{-}17)$$

Evaluating τ_s. To evaluate the interfacial shear stress τ_s, Emmons employs a relationship that was derived by Turcotte (25, Eq. 15) for the case of the transpired turbulent boundary layer on a flat plate.

---

[1] The parameter b was introduced by Turcotte into the relationship originally proposed by Rannie (28) for the case of zero mass transfer; the parameter b accounts for the fact that it is not completely clear as to whether τ_s is the correct shear stress to employ in the calculation of y^+.

Thus[1]

$$\tau_s = \tau_{s,o} \exp\left[-\frac{v_s\ 13\ 89}{(\tau_s/\rho)^{\frac{1}{2}}\ b}\right] \qquad (3\text{-}18)$$

where

$\tau_{s,o}$ = the shear stress at the wall in the absence of mass transfe

As indicated in Table 1, Eqs 3-17 and 3-18 constitute an analytical solution for the parameter β. Since Emmons misquotes and misinterprets[2] Fq. 3-18, it is of value to outline Turcotte's derivation of that equation. By combining Eqs. 3-4[3] and 3-15, Turcotte obtains the following equation for the shear stress distribution in the sublayer region. Thus

$$\tau \equiv u\left\{1 + \sinh^2\left(\frac{y^+ b}{13.89}\right)\right\}\frac{du}{dy} = \tau_s + (\rho v)_s\, u \qquad (3\text{-}19)$$

Integrating Eq. 3-19 and substituting the limit $u = 0$ at $y = 0$, one obtains the equation due to Turcotte for the velocity profile in the viscous sublayer. Thus

$$u = \frac{\tau_s}{(\rho v)_s}\left[\exp\left\{\frac{v_s}{(\tau_s/\rho)^{\frac{1}{2}}}\ \frac{13.89}{b}\ \tanh\left(\frac{y^+ b}{13\ 89}\right)\right\} - 1\right] \qquad (3\text{-}20)$$

Combining Eqs. 3-19 and 3-20, one obtains the following equation for the shear stress profile in the viscous sublayer:

---

[1] Emmons writes Eq 3-18 incorrectly He replaces the quantity $(\tau_s/\rho)^{\frac{1}{2}}$ by $(\tau_{s,o}/\rho)^{\frac{1}{2}}$ (see Ref (6), Eq B-11)

[2] See Ref (6), pp 84, 85, 91

[3] With μ replaced by $\mu + \mu_t$

$$s \exp \quad {}^{\cdot}5 \quad {}^{13\ 89}_{b} \tanh \left(\frac{y^{\cdot} b}{13\ 89} \right) \qquad (3\text{-}21)$$

Turcotte then introduces the assumption that the turbulent core external to the viscous sublayer region is unaffected by the mass transfer at the wall. Since, in the absence of mass transfer, the wall region defined by $y^+ \quad 1000$ is a constant-stress layer (18), it follows that

$$\cdot_{\lambda} = \cdot_{s,o} \qquad (3\text{-}22)$$

and that

$$\text{limit} \qquad \tanh \left(\frac{y^+}{13} \frac{b}{89} \right) = 1 \qquad (3\text{-}23)$$
$$y^+ \cdot \epsilon^+ = 25\ 4$$

Equations 3-22 and 3-23 thus reduce Eq 3-21 to Eq 3-18.

Comparison of Emmons' Analysis with the Analyses Due to Sellers, Graham, Rannie, and Knuth. Table 1, p 42, compares the analysis due to Emmons with those analyses discussed in Section 3 1.1. Column III of that table presents two analytical expressions for the paramber B under the analysis due to Emmons: (a) the expression due to Emmons (6, Eq B-19); and (b) the corrected expression derived by the writer

3 2 A Review of the Pertinent Experimental Data

The analyses reviewed in Section 3 1 are based on the premise that when the liquid film is stable, the analytical and physical models for liquid-film cooling and transpiration cooling may be considered

substantially identical. That is, the surface of the liquid film may be treated as a zero-velocity, aerodynamically smooth porous surface through which the vapor is "injected" into the adjacent boundary layer. Moreover, the concept of the viscous sublayer is introduced, that concept having been employed with success in the analysis of transpiration cooling. A review of some pertinent experimental data is presented here to demonstrate that there is a serious question regarding the validity of that premise. Discussed in Section 3.2.1 are heat-mass transfer data that indicate both the limitations of those theories reviewed in Section 3.1 and the complex nature of the phenomena that characterize the evaporation process. Data that present an explanation for anomalies that are noted in the heat-mass transfer data are discussed in Section 3.2.2.

3.2.1 Heat-Mass Transfer Data

The following items are discussed in the present section:

(a) the agreement between the heat-mass transfer rates predicted by the theory due to Knuth (8) and the data reported by Refs. (5) and (8);

(b) the physical significance of the correlation that was obtained by Emmons (6) for his experimental data; and

(c) the data obtained by Luikov (17) in an investigation of the basic phenomena that characterize the evaporation of a liquid in the presence of a "hot" gas stream.

A Comparison of Knuth's Theory with Experimental Data. Knuth observed that the average[1] heat-mass transfer rates predicted by his

[1] Averaged over the liquid-film-cooled length.

theory were significantly smaller than those he obtained experimentally, and those Kinney, et al. (5) reported; the difference was attributed by Knuth to "entrance length" effects.[1] These were not accounted for in any of the other analyses reviewed in Section 3.1. Knuth employed an empirical correction to bring the theoretical and experimental heat-mass transfer rates into agreement; that empirical correction consisted of multiplying the theoretical heat and mass transfer rates by the following expression. Thus

$$\left(1 + \frac{1}{3}\frac{d}{L} R_d^{\frac{1}{4}}\right)$$

R_d = the Reynolds number for the gas stream based on the diameter of the tube and the bulk flow parameters.

d = the diameter of the tube.

L = the liquid-film-cooled length.

Typical values of R_d and d/L for the data analyzed by Knuth were 10^6 and 10^{-1}, respectively. Hence, the empirical correction employed by Knuth was of the order of

$$1 + 1/3 \quad 10^{-1} \quad (10^6)^{\frac{1}{4}} = 2.05$$

The average heat-mass transfer rates predicted by Knuth's theory were, therefore, typically one half of those observed experimentally.

---

[1] In the experimental investigations conducted by Knuth and Kinney, et al., the velocity profile at the plane of liquid injection was essentially fully developed, whereas the temperature and concentration profiles were flat.

By way of comparison, for the case where the mass transfer is zero and the thermal boundary conditions are such that the velocity profile at the entrance to the test section is fully developed while the temperature profile is flat, the empirical correction for the "entrance length" effects is given by the following expression (8):

$$1 + 0.1 \frac{d}{L} R_d^{\frac{1}{4}}$$

where L is the length of the test section over which heat transfer occurs. Thus, if $R_d = 10^6$ and $d/L = 10^{-1}$, the ratio of the average rate of heat transfer over the test section length L to the heat transfer rate that would obtain if the temperature profile also was fully developed is

$$1 + 10^{-1} (10^6)^{\frac{1}{4}} = 1.32$$

It would appear, therefore, that the presence of the evaporating liquid film in the experimental investigations conducted by Knuth and Kinney, et al. resulted in a substantial increase in the average heat transfer rate over that which would obtain if the mass transfer was zero, that ratio being typically 2.05/1.32 = 1.55. Basic mass transfer theory, however, would predict that the "injection" of the vapor into the gas stream would act to "block" the heat transfer to the liquid film, thus reducing the observed rates of heat transfer to the film over those that would result for the case of zero mass transfer; the data for transpiration cooling presented in Fig. 3-3 in Section 3.3.2 illustrates that point. It would appear, therefore, that a significant anamolie exists in the data reported for liquid-film cooling by Refs. (5) and (8)

The Physical Significance of the Correlation Due to Emmons (6).

As noted in Table 1, the value of the parameter b with which Emmons was able to correlate his experimental data was 0.110 However, on a physical basis, Turcotte (25) argued that b must be bounded as follows:

$$1 < b < (\tau_{s,o}/\tau_s)^{\frac{1}{2}}$$

where, for transpiration cooling,

$$(\tau_{s,o}/\tau_s)^{\frac{1}{2}} > 1$$

Turcotte was able to obtain satisfactory correlation of experimental data for the transpired turbulent boundary layer by employing the median value of b; thus

$$b = \frac{1}{2}\left[1 + (\tau_{s,o}/\tau_s)^{\frac{1}{2}}\right]$$

Obviously, the value of b employed by Emmons for correlating his experimental data disagrees significantly with the values of b that are physically justified. Some of the discrepancy may be due to the incorrect quotation of Eq 3-18 by Emmons, as discussed in Section 3.1 2 It would appear, however, that a portion of the discrepancy is attributable to an incorrect assumption in his analytical model The discussion presented in the following section, Section 3 2 2, indicates that the eddy-viscosity law given by Eq 3-15, which forms the basis for Emmons' correlation, does not generally apply to the gaseous-flow regime adjacent to the surface of the liquid film

The Evaporation Data Reported by Luikov (17) The following points concerning the experimental apparatus and the experimental procedure employed in the subject investigation are worthy of note:

(a) A dry body which was internally cooled and a shallow pan--having similar overall dimensions as the dry body--containing a liquid were placed side by side on the floor of a large wind tunnel.

(b) The liquid in the evaporating pan was continuously replenished so that the free surface of the liquid was always flush with the top of the pan.

(c) Both the free surface of the liquid in the evaporating pan and the surface of the internally cooled dry body were fully instrumented with thermocouples; in all of the experiments, the rate of coolant flow through the dry body was adjusted so that the temperature of the free liquid surface and the surface of the dry body were the same

(d) Four liquids were employed in the investigation: benzol, acetone, butanol, and water.

(e) The static pressure in the wind tunnel was essentially ambient and the temperature of the main stream varied from 40 C to 120 C, and the velocities from 5 meters/sec to 14 meters/sec.

The experimental results were as follows: in all cases, the observed average heat transfer coefficient for the free liquid surface was larger than the average heat transfer coefficient for the dry body. The ratio of the two heat transfer coefficients varied from 1.2 to 1.6--the larger values corresponding to the larger evaporation rates. As indicated in the foregoing paragraphs, that trend in the experimental

data is opposed to the trend which would be predicted by mass transfer theory. Moreover, the similarity in the thermal boundary condition that was established in the subject investigation for both the dry surface and the surface of the evaporating liquid discredits to a large degree the proposal by Knuth that the disagreement between his theory and experimental liquid-film cooling data is attributable solely to "entrance length" effects.

3.2.2 Correlation of Velocity Profile Data

In the present section the data reported by Refs (19) and (21) are noted; they relate to the phenomenon of gas-liquid shear interactions in the absence of evaporative mass transfer The experimental apparatus employed in each of the subject investigations were significantly different; for a complete description of either experimental apparatus the reader is referred to the references The experimental results, however, were in qualitative agreement and may be summarized as follows When traverses were made with a pitot probe across the gas-flow regime adjacent to a "pebbled" gas-liquid interface,[1] the resultant velocity profile data correlated in the same manner as velocity profile data for rough-pipe flow It was observed that the "effective roughness" of the liquid film surface increased with increasing values of the dimensionless liquid flow rate W^+ (defined by Eq. 2-10)

Because the viscous sublayer affords the bulk of the resistance of the boundary layer to the transport of heat from a hot gas stream to a

[1] Refer to Fig 2-9, presented in Section 2-4, for a photographic definition of the "pebbled" interface structure.

solid boundary (18), and since the sublayer region becomes less influential and less well defined as the surface roughness increases (4) (18), it would appear that the interfacial phenomenon discussed above may account to a large degree for the anomalies in the heat-mass transfer data discussed in the previous section.

3.3 An Alternate Correlation for Heat-Mass Transfer Data

Consider the following recapitulation of the experimental information presented in Sections 3 2 and 2 4 For the case where the liquid film is stable, the effectiveness of liquid-film cooling apparently decreases with increasing values of the dimensionless liquid flow rate W^+, due to a corresponding increase in the "effective roughness" of the gas-liquid interface At a critical value of W^+ the inception of film instability occurs, and a further increase in W^+ causes the phenomenon of coolant entrainment which results in an even more pronounced reduction in the effectiveness of liquid-film cooling Because of these points, and since the heat transfer phenomena characterizing liquid-film cooling and transpiration cooling would appear to become progressively more similar as W^+ is decreased, the following correlation is suggested for experimental heat-mass transfer data that are obtained for liquid-film cooling Thus

$$\left(\frac{St}{St_o}\right)_{lf} = f(W^+) \left(\frac{St}{St_o}\right)_t \qquad (3\text{-}24)$$

where

$$\lim_{W^+ \to 0} f(W^+) = 1$$

The notation and subscripts in Eq. 3-24 denote the following:

St = the Stanton number for heat transfer

$f(W^+)$ = a function that must be determined experimentally.

lf - evaluated for the case of liquid film cooling

t - evaluated for the case of transpiration cooling

o - evaluated for the zero-mass transfer case

The Stanton number for heat transfer is defined by the following expression (29). Thus

$$St = \frac{q_s}{(\rho u)_e \, c_{p_e} \, (t_r - t_s)} \tag{3-25}$$

where

$$t_r = t_e + r \frac{u_e^2}{2 \, c_{p_e}} \tag{3-26}$$

= the recovery temperature for the main stream.

r = the recovery factor.

As shown by Spalding (29), the recovery factor r can be determined in most instances with sufficient accuracy from the following empirical equation due to Squire. Thus

$$r = (Pr)_*^{1/3} \tag{3-27}$$

The subscript notation $(\ )_*$ introduced in Eq 3-27 means that the subscripted quantity is to be evaluated at an appropriate reference state. The reference state suggested herein is that defined by the reference

temperature t_* due to Eckert (30), and the reference concentration $C_{v,*}$ due to Knuth (31). Thus

$$t_* = \frac{1}{2}(t_e + t_s) + r\frac{u_e^2}{2\,c_{p_e}} \qquad (3\text{-}28)$$

$$C_{v,*} = \frac{1}{2}(C_{v,e} + C_{v,s}) \qquad (3\text{-}29)^1$$

The function $f(W^+)$ in Eq. 3-24 must be determined experimentally. Procedures are outlined in Section 3.3.4 for evaluating $f(W^+)$ given either (a) bulk heat transfer data (i.e., m'_0 as a function of L for various main-stream conditions and liquid-film coolants), or, preferably, (b) the streamwise distribution of $(St)_{1f}$ as determined from detailed measurements of the structure of the boundary-layer region adjacent to the surface of the liquid film.

To facilitate implementing the correlation procedure suggested by Eq 3-24, Section 3.3.1 presents a method for obtaining an approximate evaluation of the temperature at the gas-liquid interface, and Sections 3.3.2 and 3.3.3 suggest methods for evaluating $(St/St_0)_t$ and St_0, respectively.

It should be noted that the correlation procedure developed herein differs from the semi-empirical correlations reviewed in Section 3.1 in that it is applicable to flows in the presence of pressure gradients, to the flow of a compressible fluid, and to either stable or unstable

[1] In the developments which follow, it is assumed that the concentration of the vapor in the main stream is zero. Hence, $C_{v,*} = \frac{1}{2}(C_{v,s})$.

liquid films Moreover, "entrance length" effects and streamwise variations in q_S and $(\rho v)_S$ are considered. The developments are limited, however, to the case where the gas flow is turbulent and the liquid-film coolant is non-reactive.

3.3.1 A Method for Predicting the Temperature at the Gas-Liquid Interface

The temperature at the gas-liquid interface, t_s, can be related to the bulk flow parameters by specifying (a) an interfacial energy balance, and (b) an analogy between the rates of heat and mass transfer. In the derivations that follow, the generalized energy balance given by the following equation is employed for convenience:

$$q_S = \Phi (\rho v)_S \tag{3-30}$$

The parameter Φ is defined by Eqs. 3-30 and 2-31. Thus

$$\Phi = \Delta H_v + (q_L + q_{r,L} - q_{r,S})/(\rho v)_S$$

The analogy between heat and mass transfer employed herein is that given by

$$St = St' \left(\frac{Pr}{Sc}\right)_*^{-2/3} \tag{3-31}$$

where St' is the Stanton number for mass transfer defined by

$$St' = \frac{(\rho v)_S}{(\rho u)_e} \frac{p-p_{v,s}}{p_{v,s}} \frac{R_v}{R_g} \tag{3-32}$$[1]

---

[1] Equation 3-32 also can be written in terms of the concentration of the vapor as follows (29). Thus

$$St' = \frac{(\rho v)_S}{(\rho u)_e} \frac{1-C_{v,s}}{C_{v,s}}$$

Experimental verification of the validity of Eq. 3-31 for incompressible flows is presented in Ref (32), and for compressible flows in Ref (29). It should be noted, however, that at and close to the plane where the liquid coolant is injected, Eq 3-31 is strictly applicable only if the growths of both the thermal boundary layer and the partial-pressure (or vapor-concentration) boundary layer start at that plane.

Combining Eqs 3-30, 3-31, and 3-32 yields

$$\frac{\phi}{c_{p_e}(t_r - t_s)} = \frac{p - p_{v,s}}{p_{v,s}} \frac{R_v}{R_g} \left(\frac{Pr}{Sc}\right)_*^{-2/3} \qquad (3\text{-}33)$$

In Eq 3-33 there are three unknowns: ϕ, $p_{v,s}$ and t_s Tabulated data presenting the saturation pressure of the liquid coolant as a function of its saturation temperature represents a second independent relationship for $p_{v,s}$ and t_s Thus, by specifying ϕ, t_s (or its equivalent, $p_{v,s}$) can be related to the bulk flow parameters

Figure 3-2 presents, for an air/water system, calculated values of the interface temperature t_s as a function of the static pressure p and the main-stream temperature t_e [1] The flow conditions assumed in the calculations are indicated in the figure The saturation curve for water presented in the figure illustrates the approximate error introduced by the assumption that t_s is equal to the saturation temperature for the liquid coolant under the prevailing static pressure, p, that assumption having been employed by Refs (6)(10)(11)(22)(24)

[1] The calculations were performed by employing Eq. 3-33 in conjunction with the tabulated data of Refs (32) and (33) A sample calculation is presented in Appendix B

TEMPERATURE AT INTERFACE, t_s(R)

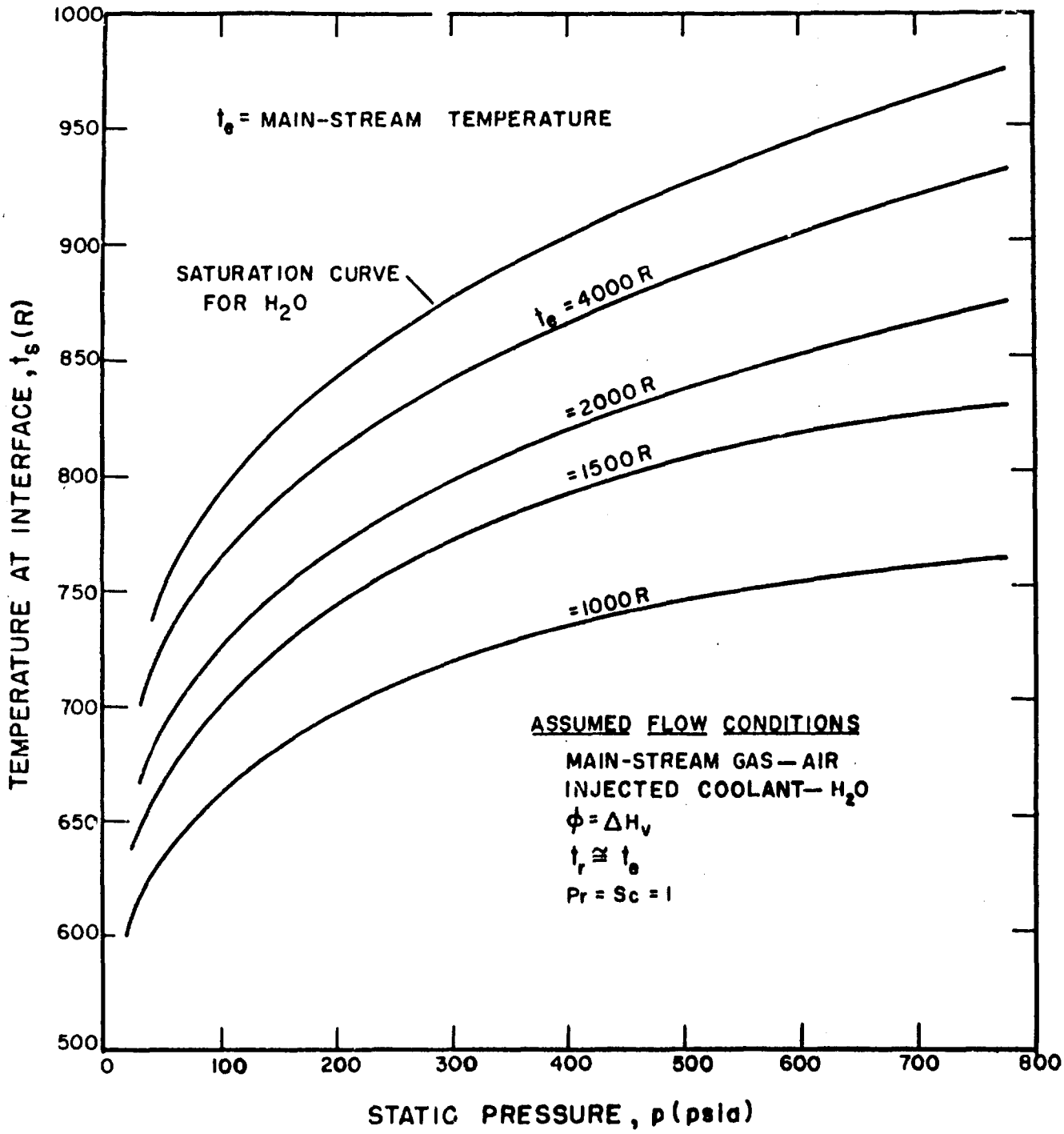

FIG. 3-2. THE TEMPERATURE AT THE INTERFACE AS A FUNCTION OF THE STATIC PRESSURE AND THE MAIN-STREAM TEMPERATURE

The calculated results presented in Fig. 3.2 agree within ± 10F with the data reported in Ref. (8) and that obtained in the preliminary investigations of liquid-film cooling conducted at the Jet Propulsion Center, Purdue University (12); the flow conditions presented in the figure apply closely to those experimental investigations. The values of p and t_e employed in the subject investigations were as follows:

Ref. (8): t_e = 1000-2300R; p = 1 atm

Ref (12): t_e = 1000K; p = 220 psia

It was stated in Section 2.2.2 that there is a question (especially for the case where a streamwise pressure gradient is imposed on the flow) regarding the fraction of the energy incident to the surface of the liquid film that is utilized for increasing the sensible enthalpy of the liquid coolant. The method presented herein for evaluating t_s affords a means by which that question can be investigated experimentally. The experimental measurement of the streamwise distribution of t_s can be related to a streamwise variation in the parameter ϕ by means of Eq. 3-33. Moreover, if the radiant and wall heat fluxes are reduced in importance, by proper design of the experimental apparatus and selection of the experimental parameters, then the definition of ϕ reduces to

ϕ = ΔH_v + (the increase in the sensible enthalpy for the liquid coolant)

Thus, for that case, the fraction of the incident heat flux utilized for increasing the sensible enthalpy of the liquid can be determined as a function of x

3.3.2 Correlation of $(St/St_o)_t$ for Transpiration Cooling

Analytically and/or experimentally it has been established satisfactorily that if transpiration cooling data are presented in the general form

$$\left(\frac{St}{St_o}\right)_t \text{ as a function of } \frac{(\rho v)_S}{(\rho u)_e} \frac{1}{St_o}$$

the resulting correlation is essentially independent of the Reynolds number for the main stream, based on the streamwise coordinate x, the Mach number for the main stream, and the ratio of the main-stream temperature to the temperature at the wall (34)(35)(36). Furthermore, the correlation is independent of the streamwise pressure gradient imposed on the flow (36). Because of the significance of those facts, such a correlation for transpiration cooling data is employed in the present developments.

Figure 3-3 presents the correlation for transpiration cooling data due to Brunner (37). The curve presented in the figure is given by the following equation. Thus

$$\left(\frac{St}{St_o}\right)_t = \left[1 + \frac{I}{St_o} \frac{(\rho v)_S}{(\rho u)_e}\right]^{-3} \tag{3-34}$$

where

$$I \quad \frac{2}{3} \left(\frac{c_{p_v}}{c_{p_e}}\right)^{0.6} \tag{3-35}$$

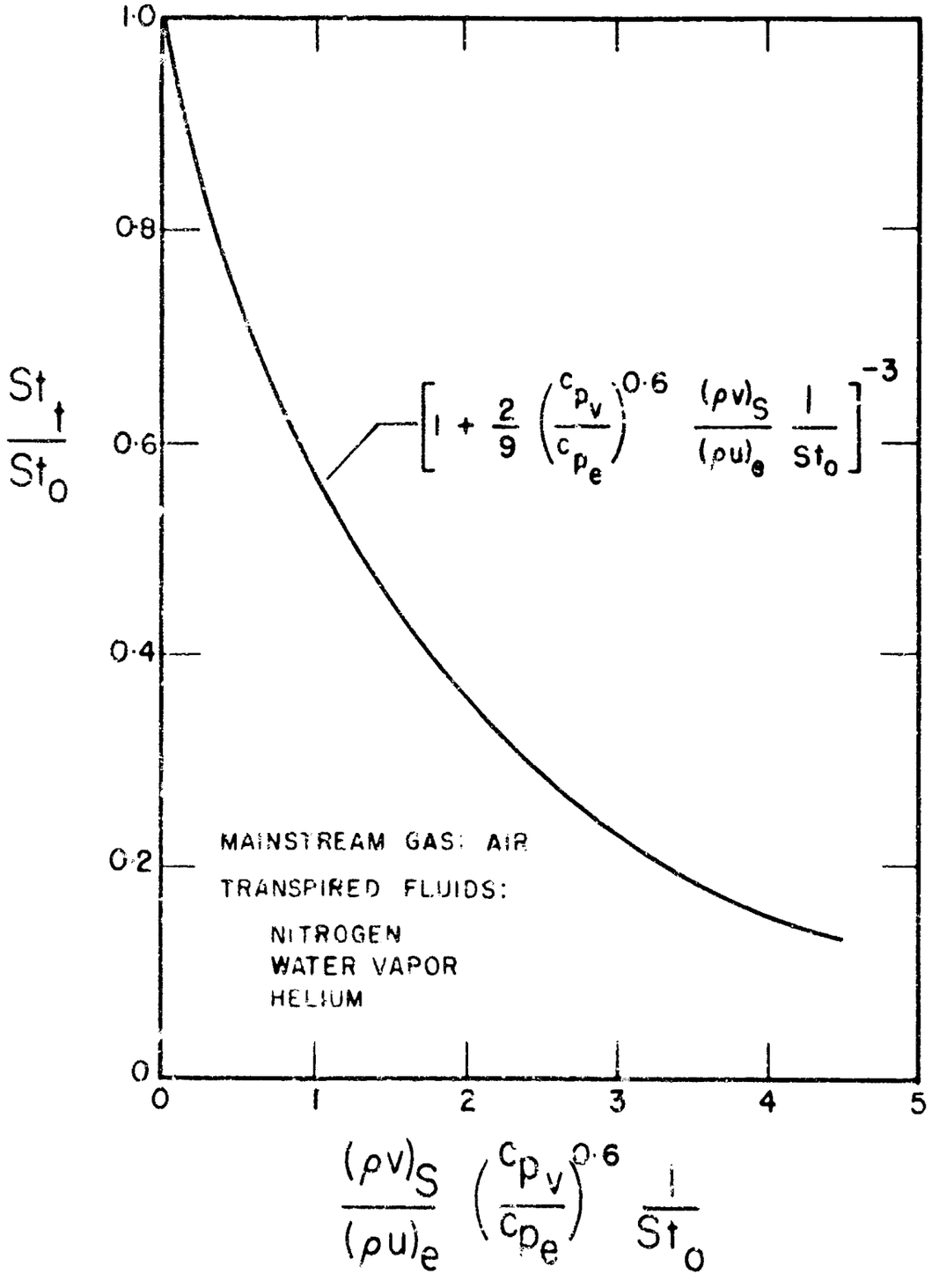

FIG. 3-3. THE CORRELATION FOR TRANSPIRATION COOLING DATA DUE TO BRUNNER (37)

The data surveyed by Brunner were for the case where either nitrogen, or helium, or water vapor is injected into an air stream. As a consequence, there is no assurance that the empirical correlation given by Eq. 3-34 is applicable to all flowing gases and injected fluids that might characterize a transpiration-cooled system. The fluids N_2, H_e, and H_2O do, however, represent a significantly wide cross section of physical property values. It appears reasonable, therefore, that Eq. 3-34 can be extended with some degree of confidence to other fluids

3.3.3 A Method for Evaluating St_o

Ideally, in an investigation of liquid-film cooling, the streamwise distribution of the Stanton number for heat transfer in the absence of mass transer, denoted by St_o, would be determined experimentally. There are, however, many instances where experimental determination of St_o is impractical. In those cases, the method suggested herein can be employed for evaluating St_o analytically

The method suggested has been developed and/or employed by numerous investigators (36)(38)(39)(40)(41). It is based on the assumption that the empirical heat-transfer law for turbulent flow over a flat plate, when written in the following form, is also applicable to turbulent flows in the presence of streamwise pressure gradients. Thus

$$St_o = St_o\,(R_\xi)$$

where

$R_\xi = \dfrac{\rho_e\, u_e\, \xi}{\mu_e}$ = the Reynolds number for the main stream based on the characteristic length ξ.

$$\xi = \int_0^t \frac{(\rho u)}{(\rho u)_e} \frac{(t_e^o - t^o)}{(t_r - t_w)} dy \qquad (3\text{-}36)$$

ξ = the energy thickness .

Δ_t = the thermal boundary layer thickness .

$t^o = t + \frac{u^2}{2c_p}$ = the stagnation temperature .

The heat-transfer law suggested in Ref. (36), and employed in the following developments, is that given by

$$St_o = 0.0128\ (Pr)^{-3/4}\ R_\xi^{-1/4} \qquad (3\text{-}37)$$

Equation 3-37 and the developments that follow can be employed to analyze a compressible gas flow by introducing the concept of the reference state, and making the following transformations for the Stanton number St_o and the Reynolds number R_ξ (42). Thus

$$St_o \rightarrow St_{o,*} \equiv \frac{\rho_e}{\rho_*}\ St_o \qquad (3\text{-}38)$$

$$R_\xi \rightarrow R_{\xi,*} \equiv \frac{\mu_e}{\mu_*}\frac{\rho_*}{\rho_e}\ R_\xi \qquad (3\text{-}39)$$

The energy integral equation is given by (38)

$$St_o = \frac{d\xi}{dx} + \xi\left[\frac{1}{u_e}\frac{du_e}{dx} + \frac{1}{(t_r - t_w)}\frac{d(t_r - t_w)}{dx} + \frac{1}{\rho_e}\frac{d\rho_e}{dx}\right] \qquad (3\text{-}40)$$

Equation 3-37 substituted into Eq. 3-40 results in an explicit equation for St_o that can be solved stepwise by numerical integration. To start the numerical calculations, however, the value of x_o and the value of

St_o at $x = x_o$ must be either known (determined experimentally) or approximated. In many applications of liquid-film cooling that are of interest, the temperature of the liquid film is significantly less than the temperature of the solid surface upstream of the plane at which film coolant is injected. In those cases, it is suggested that St_o be calculated as if the growth of the thermal boundary layer began at $x = x_o$. In other words, assume that the boundary condition $St_o = \infty$ at $x = x_o$ applies.

In the special case of an incompressible gas flow over an isothermal wall surface, Eq. 3-40 can be simplified to the form

$$St_o = \frac{\mu}{(\rho u)_e} \frac{dR_\xi}{dx} \tag{3-41}$$

Substituting Eq 3-37 into Eq 3-41, integrating the resultant expression, and imposing the limit $St_o = \infty$ at $x = x_o$, one obtains the following, relatively simple expression for St_o. Thus

$$St_o = \frac{0.02923\ Pr^{-3/5}\ R_x^{-1/5}}{\left[\frac{1}{u_e x}\int_{x_o}^{x} u_e\, dx\right]^{1/5}} \tag{3-42}$$

where

R_x $\frac{\rho_e u_e x}{\mu_e}$ = the main-stream Reynolds number based on the characteristic length x.

Equation 3-42 reduces to the following expression for the case where the main-stream velocity u_e is constant in the streamwise direction. Thus

$$St_o = 0.02923\ Pr^{-3/5}\ R_x^{-1/5}\ (1 - \frac{x_o}{x})^{-1/5} \qquad (3\text{-}43)$$

The term $(1 - \frac{x_o}{x})^{-1/5}$ in Eq. 3-43 is the correction for "entrance length" effects due to the dynamic entrance length x_o.

3.3.4 Methodology

The principal equations required for the correlation procedure suggested herein are summarized below. Thus, by definition

$$W^+ \equiv \frac{m'}{\mu_1} \qquad (2\text{-}10)$$

From the conservation of film coolant one obtains

$$m' = m'_o - \int_{x_o}^{x} (\rho v)_s\, dx \qquad (3\text{-}44)$$

Combining Eqs 3-25 and 3-30, one obtains

$$St_{1f} = \frac{(\rho v)_s}{(\rho u)_e} J \qquad (3\text{-}45)$$

where

$$J \equiv \frac{\phi}{c_{p_e}(t_r - t_s)} \qquad (3\text{-}46)$$

Furthermore, combining Eqs 3-24, 3-34, and 3-45, yields

$$\left(\frac{St}{St_o}\right)_{1f} = f(W^+) \left[1 + \frac{I}{J}\left(\frac{St}{St_o}\right)_{1f}\right]^{-3} \qquad (3\text{-}47)$$

In the discussion that follows, it is assumed that the streamwise variations for the quantities listed in Table 2 are either determined experimentally, or can be approximated from knowledge of the experimental apparatus and parameters, or can be determined analytically from the procedures presented in Sections 3.3.1 and 3.3.3.

Table 2

The Parameters That Are Considered Known As a Function of x In Outlining the Methodology

Symbol	Definition
c_{p_e}	the specific heat for the main-stream gas
c_{p_v}	the specific heat for the vapor
I	non-dimensional parameter defined by Eq. 3-35
J	non-dimensional parameter defined by Eq. 3-46
L	the liquid-film-cooled length
p	the static pressure
St_o	the Stanton number for heat transfer in the absence of mass transfer
t_e	the main-stream temperature
t_s	the temperature at the gas-liquid interface
u_e	the velocity of the main stream
x_o	the plane at which liquid-film coolant is introduced

A suggested procedure for evaluating the function $f(W^+)$ is outlined below for the following two cases: (a) the case where the streamwise

distribution of $(St)_{lf}$ is determined from detailed measurements of the structure of the boundary-layer region above the liquid film; and (b) the case where only bulk heat transfer data are obtained (i.e., m'_o as a function of L for various main-stream conditions and liquid film coolants).

Case (a): $(St)_{lf}$ Determined Experimentally The procedure for this case can be outlined as follows. Thus

(1) Determine the streamwise distribution of $(\rho v)_s$ from Eq 3-45.

(2) Determine the streamwise distribution of m' and W^+ from Eqs. 3-44 and 2-10, respectively

(3) Determine the streamwise distribution of $f(W^+)$ from Eq. 3-47.

From steps (1), (2), and (3) one obtains, for each set of input data, a plot of $f(W^+)$ as a function of W^+. Hence, for n sets of input data one obtains n such plots If the basic premise upon which the correlation suggested herein is correct, that is, if $f(W^+)$ is an universal function, each of those plots would be identical If, however, the curves differed significantly, it would indicate that the function $f(W^+)$ is not sufficient to characterize the difference between the heat transfer phenomena for liquid-film cooling and transpiration cooling However, even if that was found to be the case, if $f(W^+)$ differed from unity in any instance, the inadequacy of employing solely transpiration cooling theory in the analyses of liquid-film cooling would have been established

Case (b): m'_o and L Determined Experimentally In this case the functional form of $f(W^+)$ is assumed; i e , the function $f(W^+)$ is assumed

to be linear, exponential, etc By studying several sets of input data, it can be determined whether or not the assumed form of $f(W^+)$ was satisfactory. The complete procedure is outlined below. Thus

(1) Assume the functional form of $f(W^+)$.

(2) Determine m' and W^+ at $x = x_0$

(3) Calculate $(St)_{1f}$ at $x = x_0$, employing Eq. 3-47.

(4) Calculate $(\rho v)_S$ at $x = x_0$ by means of Eq. 3-45.

(5) Determine m' and W^+ at $x = x_0 + \Delta x$, employing Eqs. 3-44 and 2-10, respectively.

(6) Repeat steps (2) through (5), replacing $x = x_0$ by $x = x_0 + \Delta x$, and continue the reiteration until $x = x_1 = x_0 + L$.

(7) If $m' \neq 0$ at $x = x_1$, then changes must be made in step (1). To illustrate, if $f(W^+)$ was assumed to be linear in step (1), so that $f(W^+) = 1+CW^+$, then a different value must be assumed for the constant C and the computation repeated until $m' = 0$ when $x = x_1$.

For a single set of input data, regardless of the assumed functional form for $f(W^+)$, the condition $m' = o$ at $x = x_1$ will be realized By considering several sets of input data, however, it can be deduced whether that form for $f(W^+)$ satisfies the condition of universality Note that if one experiences difficulty in obtaining a form for $f(W^+)$ that simultaneously satisfies several sets of input data, it is nearly impossible to determine whether that difficulty is due to a lack of insight into the physics of the problem (i.e., the inability to "guess" at the correct $f(W^+)$), or to the fact that $f(W^+)$ does not physically exist.

4. AN ANALYSIS FOR THE GAS-VAPOR-COOLED REGION

4 1 Introduction

It is difficult, if not impossible, to make a complete mathematical analysis of the boundary-layer and heat-transfer characteristics for the region immediately downstream from the end of the liquid film. Moreover, an involved analysis generally is not warranted because of the large number of assumptions that must be made concerning the velocity and temperature profiles, the form factor, the skin-friction law, the heat-transfer law, etc As a consequence of this fact, the analysis presented herein is based on an idealized and relatively simple flow model

Both Emmons (6) and Guinn (7) developed semi-empirical analyses for the gas-vapor-cooled region; those analyses were based on the flow model suggested by Hatch and Papell (43) for gas-film cooling The analysis presented here differs from those due to Emmons and to Guinn in the following respects: (a) boundary-layer flow rather than fully-developed-pipe flow is considered; and (b) the analysis is generalized so that it can be applied to a compressible gas flow in the presence of a streamwise pressure gradient The analysis is dependent, however, on the analysis for the liquid-film-cooled region presented in Section 3.3.

As discussed in Section 2.1.2, a complete analysis for the gas-vapor-cooled region requires the consideration of two cases: (a) the case where the wall is adiabatic; and (b) the case where the wall is externally cooled. Those two cases are considered in Sections 4.2 and 4.3, respectively.

4.2 The Case Where the Wall is Adiabatic

4.2.1 The Flow Model

The flow model employed for the analysis of the gas-vapor-cooled region is defined by the following conditions

(1) The wall is adiabatic.

(2) The boundary layer flow is fully turbulent.

(3) The thermal, the diffusional, and the dynamic boundary layer thicknesses are equal; the latter is denoted by $y = \Delta$.

(4) The stagnation enthalpy for the main stream, denoted by h_e^o, is a constant in the streamwise direction; the stagnation enthalpy for the gas stream is defined, in general, by

$$h^o = c_p t + \frac{u^2}{2} \tag{4-1}$$

(5) The velocity profile and the stagnation-enthalpy profile for the boundary layer are of the functional forms

$$\frac{u}{u_e} = f_1\left(\frac{y}{\Delta}\right) \tag{4-2}$$

and

$$\frac{h^o - h_{aw}}{h_e^o - h_{aw}} = f_2\left(\frac{y}{\Delta}\right) \tag{4-3}$$

where h_{aw} is the enthalpy for the fluid adjacent to the adiabatic wall. To illustrate, f_1 could be assumed of the power-law form:

$$f_1 = \left(\frac{y}{\Delta}\right)^{\frac{1}{n}} \tag{4-4}$$

In addition, f_2 could be assumed of the form

$$f_2 = A + B\left(\frac{y}{\Delta}\right) + C\left(\frac{y}{\Delta}\right)^2 + D\left(\frac{y}{\Delta}\right)^3 \tag{4-5}$$

The constants in Eq. 4-5 can be evaluated from the following boundary conditions that apply to f_2. Thus

$$f_2(0) = 0$$

$$f_2(1) = 1$$

$$\frac{\partial f_2}{\partial y}(0) = 0$$

$$\frac{\partial f_2}{\partial y}(1) = 0$$

The resultant expression for f_2 is

$$3\left(\frac{y}{\Delta}\right)^2 - 2\left(\frac{y}{\Delta}\right)^3 \tag{4-6}$$

For the present analysis, however, the actual forms of f_1 and f_2 need not be assumed, only the assumption that f_1 and f_2 exist for the gas-vapor-cooled region is required.

4 2.2 The Energy Balance

Figure 4-1 presents, schematically, a control volume for the gas-vapor-cooled region; the control surface for that control volume is defined by $x = x_1$, $x = x$, $y = \delta$, and $y = o$. The following energy fluxes, written in accordance with the flow model defined in the foregoing section, are presented in the figure:

(a) $\int_0^{\delta} \rho u h^o \, dy$ = the rate at which thermal and kinetic energy is transferred into the control volume per unit spanwise length at the station $x = x_1$.

(b) $\int_0^{\delta} \rho u h^o \, dy$ = the rate at which thermal and kinetic energy is transferred out of the control volume per unit spanwise length at the station $x = x$

(c) $(m'' - m''_1)h_e^o$ = the rate at which thermal and kinetic energy is transferred from the main stream into the control volume per unit spanwise length

The parameter m'' in term (c) is defined as follows:

$$m'' = \int_0^{\delta} \rho u \, dy \qquad (4\text{-}7)$$

= the rate at which mass is transferred through the boundary layer per unit spanwise length at the station $x = x$.

The energy balance for the control volume in Fig 4-1 can be written as follows Thus

$$\int_0^{\delta_1} \rho u h^o \, dy + (m''-m''_1)\, h_e^o = \int_0^{\delta} \rho u h^o \, dy \qquad (4\text{-}8)$$

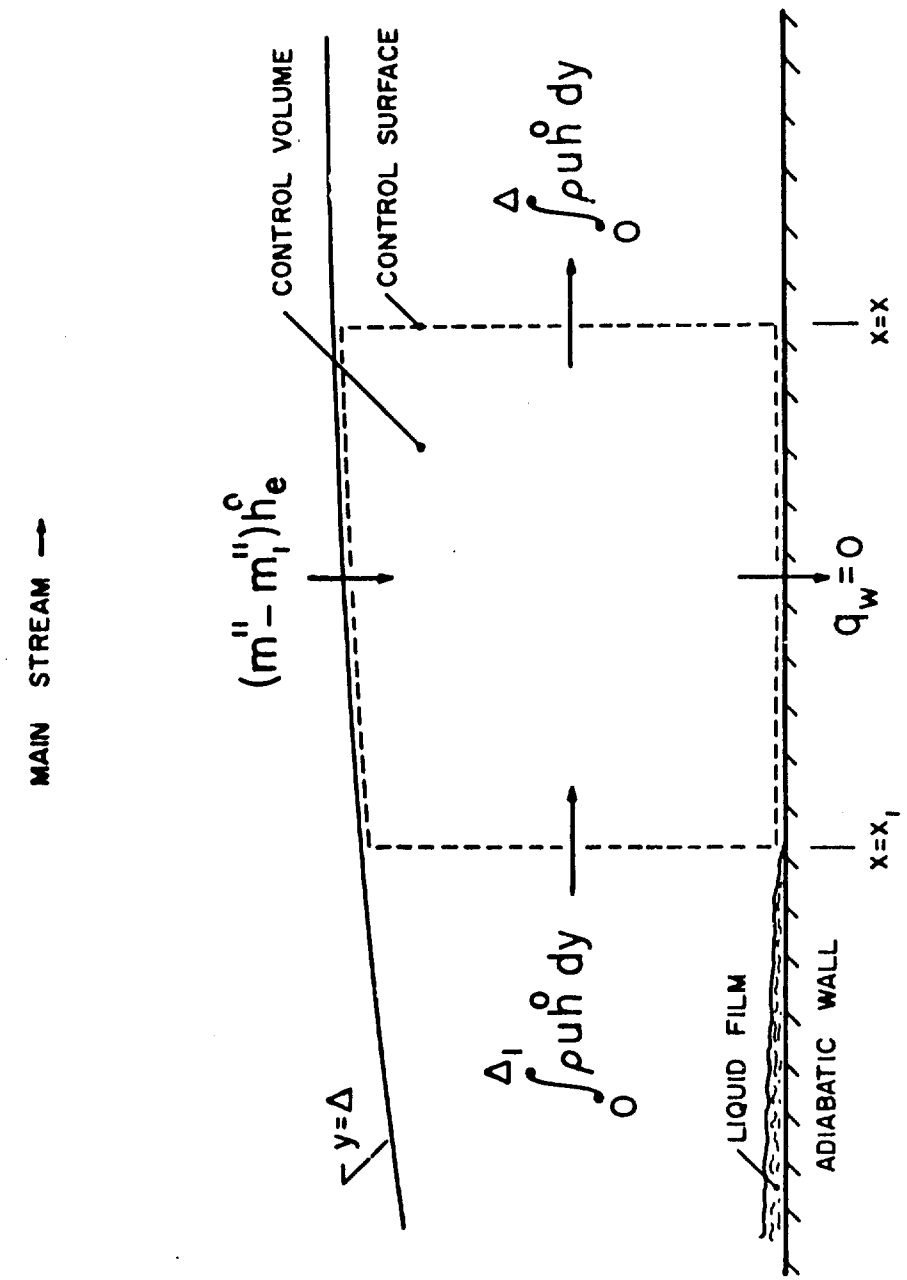

FIG. 4-1. THE CONTROL VOLUME FOR THE GAS-VAPOR-COOLED REGION

Employing Eq. 4-7, Eq. 4-8 can be written in the form

$$m''_1 \frac{\int_0^{\Delta_1} \rho u h^o \, dy}{\int_0^{\Delta_1} \rho u \, dy} + (m''-m''_1) h_e^o = m'' \frac{\int_0^{\Delta} \rho u h^o \, dy}{\int_0^{\Delta} \rho u \, dy} \qquad (4\text{-}9)$$

In order to realize the desired simplicity of the present analysis, the following approximation is introduced concerning the integral terms in Eq. 4-9. Thus[1]

$$\frac{\int_0^{\Delta} \rho u h^o \, dy}{\int_0^{\Delta} \rho u \, dy} \cong \frac{\int_0^{\Delta} u h^o \, dy}{\int_0^{\Delta} u \, dy}$$

Thus, Eq. 4-9 can be written in the following form by introducing that approximation and Assumption (5) of the flow model:

$$m''_1 \frac{\int_0^{\Delta_1} f_1 \{(h_e^o - h_{aw,1}) f_2 + h_{aw,1}\} \, dy}{\int_0^{\Delta_1} f_1 \, dy} + (m''-m''_1) h_e^o =$$

$$m'' \frac{\int_0^{\Delta} f_1 \{(h_e^o - h_{aw}) f_2 + h_{aw}\} \, dy}{\int_0^{\Delta} f_1 \, dy}$$

The latter expression can be rewritten in the form

---

[1] Note that this approximation is not equivalent to and is less restrictive than the assumption of constant density.

$$m''_1 (h_e^o - h_{aw,1}) - m''_1 (h_e^o - h_{aw,1}) \frac{\int_0^1 f_1 f_2 \, d(\frac{y}{\Delta})}{\int_0^1 f_1 \, d(\frac{y}{\Delta})} =$$

$$m'' (h_e^o - h_{aw}) - m'' (h_e^o - h_{aw}) \frac{\int_0^1 f_1 f_2 \, d(\frac{y}{\Delta})}{\int_0^1 f_1 \, d(\frac{y}{\Delta})} \qquad (4\text{-}10)$$

Finally, the terms in Eq 4-10 can be combined to yield the following energy balance for the control volume presented in Fig. 4-1. Thus

$$\frac{h_e - h_{aw}}{h_e^o - h_{aw,1}} = \frac{m''_1}{m''} \qquad (4\text{-}11)$$

The relatively simple form of Eq. 4-11 is due principally to Assumption (5) of the flow model.

Equation 4-11 enables the determination of the enthalpy for the fluid adjacent to the adiabatic wall as a function of x once h_e^o and $h_{aw,1}$ and m'' as functions of x are known. The parameter h_e^o is normally known from the statement of the problem, and the parameter $h_{aw,1}$ can be determined from the developments presented in Section 3.3.1. The evaluation of m'' as a function of x is considered in Section 4.2.3.

To evaluate the temperature distribution for the adiabatic wall from the distribution of h_{aw}, the specific heat for the fluid adjacent to the wall must be known. Excluding the region close to the station $x = x_1$, it is sufficiently accurate to take that specific heat to be

that for the main-stream gas because of the low concentration of the vapor in comparison to that of the main-stream gas. Moreover, since the temperature of the adiabatic wall at $x = x_1$ can be independently determined from the developments of Section 3.3.1, it follows that the adiabatic-wall temperature distribution for the entire gas-vapor-cooled region can be determined with sufficient accuracy once h_{aw} as a function of x is known.

4.2.3 The Evaluation of m"

Equation 4-5, which defines the parameter m", can be rewritten in the form

$$m'' = (\rho u)_e \left(\frac{\Delta}{\theta} - \frac{\Delta^*}{\theta}\right) \theta \qquad (4\text{-}12)$$

where

$$\Delta^* \equiv \int_0^{\Delta} \left(1 - \frac{\rho u}{(\rho u)_e}\right) dy = \text{the displacement thickness.} \qquad (4\text{-}13)$$

$$\theta \equiv \int_0^{\Delta} \frac{\rho u}{(\rho u)_e} \left(1 - \frac{u}{u_e}\right) dy = \text{the momentum thickness.} \qquad (4\text{-}14)$$

Equation 4-12 shows that m" can be determined as a function of x if Δ/θ, Δ^*/θ, and θ are known as functions of x. The evaluation of those quantities is considered in the following paragraphs.

The Evaluation of Δ/θ and Δ^*/θ. Persh and Lee (44) have tabulated the values of Δ/θ and Δ^*/θ as functions of the main-stream Mach number and the wall-to-main-stream temperature ratio. It is suggested, therefore, that these tabulated data be employed for evaluating Δ/θ and Δ^*/θ when the variation in the density for the gas stream across the

boundary layer is significant. If, however, that density variation is not significant, it is suggested that the subject parameters be calculated by applying the power-law velocity profile (see Eq. 4-4). The resultant expressions for Δ/θ and Δ^*/θ are (4, p. 536)

$$\frac{\Delta}{\theta} = \frac{(1+n)(2+n)}{n} \tag{4-15}$$

and

$$\frac{\Delta^*}{\theta} = \frac{(2+n)}{n} \tag{4-16}$$

The Evaluation of θ. To determine the value of the momentum thickness θ as a function of x, one must solve the momentum integral equation. That equation can be written in the form (45)

$$\frac{c_f}{2} = \frac{d\theta}{dx} + \theta \left[\left(2+\frac{\Delta^*}{\theta}\right) \frac{1}{u_e} \frac{du_e}{dx} + \frac{1}{\rho_e} \frac{d\rho_e}{dx} \right] \tag{4-17}$$

Or in the form (46)

$$\frac{c_f}{2} = \frac{d\theta}{dx} + \theta \left[\frac{1}{M} \frac{dM}{dx} \frac{\left[(\Delta^*/\theta) + 2 - M^2\right]}{\left(1 + \left(\frac{\lambda-1}{2}\right) M^2\right)} \right] \tag{4-18}$$

The notation for Eqs. 4-17 and 4-18 is as follows:

$$\frac{c_f}{2} = \frac{\tau_w}{\rho_e u_e^2} = \text{the skin-friction coefficient.} \tag{4-19}$$

M = the Mach number for the main-stream flow.

$\lambda = \frac{c_p}{c_v}$ = the specific heat ratio.

To solve[1] either Eq. 4-17 or Eq. 4-18 for θ, one must specify the form of the skin-friction law; the latter is denoted functionally by

$$\frac{c_f}{2} = \frac{c_f}{2}(R_\theta)$$

where

$$R_\theta \equiv \frac{\rho_e u_e \theta}{\mu_e} = \text{the Reynolds number for the main stream based on the characteristic length } \theta. \qquad (4\text{-}20)$$

Furthermore, the boundary condition on θ at the station $x = x_1$, denoted by θ_1, also must be specified before θ as a function of x can be determined from either Eq. 4-17 or Eq. 4-18.

Several empirical skin-friction laws are presented in Chapter 22 of Ref. (4) for the case where the gas flow is turbulent, incompressible, and over a flat plate. In the analysis of gas flows with pressure gradients (particularly favorable pressure gradients), it is common to assume that the skin-friction law is that established empirically for the flat-plate case (45)(46)(4). Furthermore, the case where the gas flow is compressible can be analyzed by introducing the following transformations into the form of the skin-friction law for incompressible flow (42):

$$\frac{c_f}{2} \rightarrow \left(\frac{c_f}{2}\right)_\star \equiv \frac{\rho_e}{\rho_\star} \frac{c_f}{2} \qquad (4\text{-}21)$$

and

---

[1] A numerical solution is generally required for either Eq. 4-17 or 4-18.

$$R_\theta \rightarrow R_{\theta,*} \equiv \frac{\rho_*}{\rho_e} \frac{\mu_e}{\mu_*} R_\theta \tag{4-22}$$

The reference state denoted by $(\ )_*$ in Eqs. 4-21 and 4-22 was discussed in Section 3.3. It is suggested that, in evaluating the physical properties, the composition of the gas be assumed uniform throughout the boundary layer and equal to that for the main stream; i.e., assume that the reference temperature given by Eq 3-28 is sufficient to define the reference state

A sufficiently accurate approximation to θ_1 can be obtained in the following manner First, assume that the Colburn analogy, given by the following equation, applies at $x = x_1$ Thus

$$(St)_{1f} = \frac{c_f}{2} (Pr)_*^{-2/3} \tag{4-23}$$

Then, employing the skin-friction law which relates $\frac{c_f}{2}$ and θ, one can approximate the value of θ_1 once $(St)_{1f}$ at $x = x_1$ has been determined from the analysis presented in Section 3 3 for the liquid-film-cooled region

4 2 4 A Special Case

To illustrate the developments presented in the foregoing, consider the special case defined by the following conditions

1 The gas flow is incompressible, constant-density, and over an adiabatic flat plate

2 The skin-friction law is that due to Prandtl (4, Eq 22 7). Thus

$$\frac{c_f}{2} = 0.0128\, R_\theta^{-1/4} \tag{4-24}$$

3. The velocity profile for the boundary layer is given by

$$\frac{u}{u_e} = \left(\frac{y}{\Delta}\right)^{1/7} \tag{4-25}$$

4. The specific heat for the vapor and for the main-stream gas are equal and are not functions of temperature

For that special case, Eq 4-11 reduces to the form

$$\frac{t_e - t_{aw}}{t_e - t_{aw,1}} = \frac{m''_1}{m''} \tag{4-26}$$

Equation 4-12 reduces to (refer to Eqs. 4-15 and 4-16)

$$m'' = 9\, \rho u_e\, \theta \tag{4-27}$$

Equation 4-17 simplifies to the form

$$\frac{c_f}{2} = \frac{d\theta}{dx} = \frac{dR_\theta}{dR_x} \tag{4-28}$$

where

$R_x = \frac{\rho u_e}{\mu} x$ = the Reynolds number for the main stream based on the characteristic length x (4-29)

Upon combining Eqs 4-26 and 4-27, one obtains

$$\frac{t_e - t_{aw}}{t_e - t_{aw,1}} = \frac{\theta_1}{\theta} = \frac{R_{\theta_1}}{R_\theta} \tag{4-30}$$

In addition, substitution of Eq. 4-24 into Eq. 4-28 yields

$$0\ 0128\ dR_x = R_\theta^{1/4}\ d\ R_\theta \tag{4-31}$$

Integrating Eq. 4-31 and substituting the limit $R_\theta = R_{\theta_1}$ at $x = x_1$, one obtains

$$R_\theta^{5/4} = 0.016\ R_x\ (1 - \frac{x_1}{x}) + R_{\theta_1}^{5/4} \tag{4-32}$$

It follows from Eq. 4-30 and Eq. 4-32 that for the special case in question, the adiabatic-wall temperature as a function of x is given in non-dimensional form by the following equation. Thus

$$\frac{t_e - t_{aw}}{t_e - t_{aw,1}} = \frac{R_{\theta_1}}{[0.016\ R_x(1-\frac{x_1}{x}) + R_{\theta_1}^{5/4}]^{4/5}} \tag{4-33}$$

Finally, to complete the solution, R_{θ_1} can be related to $(St)_{1f,1}$, the Stanton number for heat transfer at $x = x_1$, by combining Eqs. 4-21 and 4-24. The resultant expression is

$$R_{\theta_1} = \left[\frac{(St)_{1f,1}}{0.0128}^{2/3}\right]^4 \tag{4-34}$$

4.3 The Case Where the Wall is Cooled Externally

For the subject case, the basic analytical problem is that of relating the local values for the wall temperature and the wall-heat flux to the main-stream conditions. It can be inferred from several mass-transfer cooling (and heating) studies reported in the literature (Refs. 47-51) that heat-transfer data that are obtained for the gas-vapor-cooled region should correlate satisfactorily in the following manner Thus

$$St_{gv} = St_o \frac{t_{aw} - t_w}{t_e^o - t_w} \tag{4-35}$$

where

$$St_{gv} \quad \frac{q_w}{(\rho u)_e (t_{aw}-t_w)} \tag{4-36}$$

St_{gv} = the Stanton number for heat transfer for the gas-vapor-cooled region

St_o = the Stanton number for heat transfer in the absence of gas-vapor cooling.

t_{aw} = the temperature the wall would obtain if it was adiabatic.

t_w = the temperature the wall obtains due to the fact that it is cooled externally

q_w = the heat flux from the hot gas stream to the external coolant

Equation 4-35, together with the developments presented in Sections 4-2 and 3 3 3, which enable the determination of t_{aw} and St_o[1] as functions of x, respectively, thus represents the solution for the subject case

[1] It is important to note that in the evaluation of St_o in Eq. 4-35, the boundary condition $St_o = \infty$ at $x = x_1$ applies (47-51).

5 CONCLUSIONS AND RECOMMENDATIONS

Having studied the physical and theoretical nature of liquid-film cooling, together with the pertinent literature, the following general conclusions are drawn:

1 The feasibility of liquid-film cooling a rocket thrust chamber has been established experimentally (5)(6)(8)(10)(11)(52)(53)(54). However, the fundamental phenomena characterizing that process are not well understood. In particular, the interfacial phenomena (film instability, droplet entrainment, and the "effective" film roughness) are not well defined, especially for the case where the pressure and/or main-stream temperature is substantially greater than ambient. It is generally agreed, however, that those phenomena significantly influence the effectiveness of liquid-film cooling.

2 A need exists for accurate heat-mass transfer data for the liquid-film-cooled region, especially for the case characterized by one or more of the following conditions: (a) the gas flow is compressible; (b) a pressure gradient is imposed on the flow; and (c) a film coolant other than water is employed.

3 The analyses presented to date for liquid-film cooling have either lacked agreement with the experimental data or have resulted in correlations that are not justified physically. Obviously, further experimental evaluation of the basic phenomena would enable the postulation of more

realistic analytical models and the development of more complete analyses

4 Additional experimental investigation of the gas-vapor-cooled region is needed Boundary layer measurements would aid in defining the mixing characteristics for that region, and would enable the postulation of a more realistic flow model than those postulated previously (6)(7), and that presented in the subject report

In view of the aforementioned conclusions, and in accordance with the foregoing developments presented in the subject report, some recommendations for further research are presented below:

1. Conduct cold-flow studies (i.e , zero evaporative mass transfer) of film instability and entrainment to determine the influence, if any, of the dimensionless liquid flow rate W_0^+, the dimensionless film thickness δ_f^+, the Reynolds number for the gas stream, the pressure, etc on those phenomena For these studies, and for those recommended below, several fluids in addition to water should be studied, and pressures significantly greater than ambient should be employed.

2 Conduct additional cold-flow studies utilizing a pitot probe to determine the velocity profile across the boundary layer as a function of x Use these data to study the "effective" roughness of the gas-liquid interface

3 Conduct heat-mass transfer studies to obtain data that can be employed to evaluate the correlation procedure suggested in Section 3 3 Initial studies should be conducted to obtain bulk heat-mass transfer

data for a significantly wide range of experimental parameters. Subsequently, more sophisticated studies should be conducted to obtain boundary layer data that would aid in the understanding of the phenomena occurring at the gas-liquid interface

4. Experimentally investigate the region downstream of the liquid film for the case where the wall is adiabatic. Initial studies should be conducted wherein only the wall temperature distribution and the bulk flow parameters are determined. Those data can be employed to evaluate the analysis presented in Section 4.2. Subsequently, experimental studies should be conducted to obtain boundary layer measurements that would aid in the postulation of a realistic flow model for the subject wall region.

6 BIBLIOGRAPHY

1 Coulbert, C. D , "Selecting Cooling Techniques for Liquid Rockets for Spacecraft," Journal Spacecraft and Rockets, March-April 1964.

2. Kramer, E L., and S. Gronich, "A Transpiration-Cooled Nozzle as Applied to a Gas-Core Nuclear Propulsion System," Journal Spacecraft and Rockets, May-June 1965.

3 Benser, W A., and R W Graham, "Hydrogen Convective Cooling of Rocket Nozzles," ASME Paper 62-AV-22 (1962).

4. Schlichting, H , "Boundary Layer Theory," Fourth Edition, McGraw-Hill, Inc , New York, 1960

5 Kinney, G R , A E Abramson, and J L Sloop, "Internal-Liquid-Film-Cooling Experiments with Air-Stream Temperatures to 2000° F in 2- and 4-Inch Diameter Horizontal Tubes," NACA Report 1087 (1952)

6 Emmons, D L , "Effects of Selected Gas Stream Flow Parameters and Coolant Physical Properties on Film Cooling of Rocket Motors," PhD Thesis, Purdue University, Lafayette, Indiana, August 1962

7. Guinn, G R., "The Influence of Dual Injection Slots on the Film Cooling of Rocket Motor Combustion Chambers," MSME Thesis, Purdue University, January 1963

8 Knuth, E L., "The Mechanics of Film Cooling--Part 2," Jet Propulsion, January 1955

9 Crocco, L., "An Approximate Theory of Porous, Sweat, or Film Cooling with Reactive Fluids," Journal American Rocket Society, November-December 1952.

10. Graham, A R., "Film Cooling of Rocket Motors, Part I An Experimental and Theoretical Investigation of Film Cooling of Rocket Motors," PhD Thesis, Jet Propulsion Center, Purdue University, Lafayette, Indiana, January 1958

11. Sellers, J. P , "Experimental and Theoretical Study of the Application of Film-Cooling to a Cylindrical Rocket Thrust Chamber," PhD Thesis, Purdue University, Lafayette, Indiana, June 1958

12. An experimental investigation of liquid-film cooling currently being conducted at the Jet Propulsion Center, Purdue University, under the auspices of the Office of Naval Research, Power Branch, under contract Nonr 1100 (21)

13. Knuth, E. L., "Evaporation from Liquid Wall Films into a Turbulent Gas Stream," 1953 Heat Transfer and Fluid Mechanics Institute, Stanford University Press, Stanford, California.

14. Knuth, E. L , "The Mechanics of Film Cooling--Part I," Jet Propulsion, November-December 1954

15. Taylor, N. H., G. F Hewitt, and P. M C. Lacey, "The Motion and Frequency of Large Disturbance Waves in Annular Two-Phase Flow of Air-Water Mixtures," Chemical Engineering Science, August 1963.

16. Luikov, A. V., "Heat and Mass Transfer in Evaporation," International Chemical Engineering, April 1963.

17. Luikov, A. V., "Heat and Mass Transfer in Capillary-Porous Bodies," Advances in Heat Transfer, 1964, Edited by T. F Irvine and J. P. Hartnett, Academic Press, New York

18. Kestin, J , and P D. Richardson, "Heat Transfer Across Turbulent, Incompressible Boundary Layers," Journal Heat and Mass Transfer, June 1963.

19. Hanratty, T. J , and J M Engen, "Interaction Between a Turbulent Air Stream and a Moving Water Surface," A I Ch E. Journal, September 1957.

20 Graham, A R., and M J Zucrow, "Some Considerations of Film Cooling for Rocket Motors," Jet Propulsion, June 1957.

21. Gill, L. E , G F Hewitt, and P. M C Lacey, "Sampling Probe Studies of the Gas Core in Annular Two-Phase Flow--II Studies of the Effect of Phase Flow Rates on Phase and Velocity Distribution," Chemical Engineering Science, September 1964

22 Zucrow, M J , and J P Sellers, "Experimental Investigation of Rocket Motor Film Cooling," Journal American Rocket Society, May 1961

23. Rannie, W D , "A Simplified Theory of Porous Wall Cooling," Progress Report No 4-50 Jet Propulsion Laboratory, California Institute of Technology, Pasadena, California, November 1947.

24 Kinney, G. R , and A. E Abramson, "Investigation on Annular Liquid Flow with Co-Current Air Flow in Horizontal Tubes," NACA RM E51C13, May 1951.

25 Turcotte, D. L., "A Sublayer Theory for Fluid Injection Into the Incompressible Turbulent Boundary Layer," Journal Aerospace Sciences, September 1960

26. Graham, A. R., "Film Cooling of Rocket Motors, Part II. Film Cooling, Its Theory and Application," PhD Thesis, Jet Propulsion Center, Purdue University, Lafayette, Indiana, January 1958.

27. Reynolds, O., "On the Extent and Action of the Heating Surface of Steam Boilers," Proceedings of the Literary and Philosophical Society of Manchester, Vol 14, 1874 Reprinted in "Scientific Papers of Osborne Reynolds," Vol 1, Cambridge University Press, New York, 1900, pp 81-85.

28. Rannie, W D., "Heat Transfer in Turbulent Shear Flow," Aeronautical Sciences, May 1956.

29. Spalding, D. B., D M Auslander, and T. R. Sundaram, "The Calculation of Heat and Mass Transfer Through the Turbulent Boundary Layer on a Flat Plate at High Mach Numbers, with and without Chemical Reaction," Supersonic Flow, Chemical Processes and Radiative Transfer, Edited by D B Olfe and V Zakkay, Pergamon-MacMillan, 1964, pp. 211-276

30. Eckert, E. R G., "Engineering Relations for Friction and Heat Transfer to Surfaces in High Velocity Flow," Journal Aerospace Sciences, August 1955

31. Knuth, E. L , "On Two Alternate Motivations of Reference-State Expressions for Turbulent Flows with Mass Transfer," AIAA Journal, May 1963

32. Eckert, E. R G , and R M Drake, Jr , "Heat and Mass Transfer," McGraw-Hill Book Company, Inc , New York, 1959

33 Keenan, J H., and F G Keyes, "Thermodynamic Properties of Steam," First Edition, John Wiley and Sons, Inc., New York, 1936.

34 Bartle, E. R., and B M Leadon, "Experimental Evaluation of Heat Transfer with Transpiration Cooling in a Turbulent Boundary Layer at M = 3 2," Journal Aerospace Sciences, January 1960

35 Rubesin, M. W , "An Analytical Estimation of the Effect of Transpiration Cooling on the Heat Transfer and Skin Friction Characteristics of a Compressible, Turbulent Boundary Layer," NACA TN 3341, December 1954

36 Romanenko, P. N , and V N. Kharchenko, "The Effect of Transverse Mass Flow on Heat Transfer and Friction Drag in a Turbulent Flow of Compressible Gas Along an Arbitrarily Shaped Surface," Journal Heat and Mass Transfer,

37. Brunner, M. J., "Transpiration Cooling Tests of a Sharp, Sphere-Cone in a Rocket Exhaust Using N_2, He, and H_2O Coolants," ASME paper No. 64-WA/HT-50 (1964).

38. Romanenko, P. N., A. I. Leontev, and A. N. Oblivis, "Investigation on Resistance and Heat Transfer of Turbulent Air Flow in Axisymmetrical Channels with Longitudinal Pressure Gradient," Journal Heat and Mass Transfer, June 1962.

39. Ambrok, G. S., "Approximate Solution of Equations for the Thermal Boundary Layer with Variations in Boundary Layer Structure," Soviet Technical Physics, September 1957.

40. Mayer, E., "Analysis of Convective Heat Transfer in Rocket Nozzles," Journal American Rocket Society, July 1961.

41. McCuen, P. A., R. E. Lundberg, and J. W. Schaefer, "A Study of Solid-Propellant Rocket Motor Exposed Materials Behavior, Second Quarterly Progress Report," Vidya Report RTD-TDR-63-1076, November 1963.

42. Coles, D , "The Turbulent Boundary Layer in a Compressible Fluid," Physics of Fluids, September 1964.

43. Hatch, J. E and S. S. Papell, "Use of a Theoretical Flow Model to Correlate Data for Film Cooling or Heating an Adiabatic Wall by Tangential Injection of Gases of Different Fluid Properties," NASA TN D-130, November 1959.

44. Persh, J., and R. Lee, "A Method for Calculating Turbulent Boundary Layer Development in Supersonic and Hypersonic Nozzles Including the Effects of Heat Transfer," U S Naval Ordnance Lab. Report 4200, 1956.

45. Bartz, D. R , "An Approximate Solution of Compressible Turbulent Boundary-Layer Development and Convective Heat Transfer in Convergent-Divergent Nozzles," ASME Trans , November 1955.

46. Elliot, D G , D R Bartz, and S Silver, "Calculation of Turbulent Boundary-Layer Growth and Heat Transfer in Axi-Symmetric Nozzles," Jet Propulsion Lab TR 32-387, February 1963.

47. Librizzi and R J. Cresci, "Transpiration Cooling of a Turbulent Boundary Layer in an Axisymmetric Nozzle," AIAA Journal, April 1964.

48. Libby, P A , and R. J Cresci, "Experimental Investigation of the Downstream Influence of Stagnation Point Mass Transfer," Journal Aerospace Sciences, January 1961.

49 Seban, R A , "Heat Transfer and Effectiveness for a Turbulent Boundary Layer with Tangential Fluid Injection," ASME Paper No. 59-A-177 (1960)

50 Seban, R. A., and L. H. Back, "Effectiveness and Heat Transfer for a Turbulent Boundary Layer with Tangential Injection and Variable Free-Stream Velocity," Journal Heat Transfer, August 1962

51 Hartnett, J. P , R. C. Birkebak, and E R G Eckert, "Velocity Distributions, Temperature Distributions, Effectiveness and Heat Transfer for Air Injected Through a Tangential Slot Into a Turbulent Boundary Layer," Journal Heat Transfer, August 1961

52 Shurman, G A , "On Investigation of Film Cooling a Flame Tube," Progress Report No 1-74, Jet Propulsion Laboratory, California Institute of Technology, Pasadena, California, June 1948

53 Boden, R. H., "Heat Transfer in Rocket Motors and the Application of Film and Sweat Cooling," ASME Paper No. 50-A-53 (1950).

54. Abramson, A. E , "Investigation of Internal Film Cooling of an Exhaust Nozzle of a 1000-pound-Thrust Liquid-Ammonia-Liquid-Oxygen Rocket Engine," NACA RM E52C26 (1952).

APPENDICES

APPENDIX A

NOTATION

C_i	specific concentration of "i" species
$\frac{c_f}{2}$	skin friction coefficient (Eq. 4-19)
c_p	specific heat at constant pressure
c_v	specific heat at constant volume
d	tube diameter
D	diffusion coefficient
f	denotes a function
h	specific enthalpy
h'	heat transfer coefficient
h^o	stagnation enthalpy (Eq 4-1)
ΔH_v	latent heat of vaporization
I	See Equation 3-35
J	See Equation 3-46
k	thermal conductivity
L	liquid-film-cooled length
m'	rate of liquid coolant flow/unit spanwise length (Eq 2-7)
m"	rate of gas flow through the boundary layer/unit spanwise length (Eq 4-7)

M	Mach number
n	parameter in the power-law velocity profile (see Eq. 4-4)
p	static pressure
p_i	partial pressure for "i" species
Pr	Prandtl number = $\frac{\mu c_p}{k}$
Pr_t	turbulent Prandtl number = $\frac{\mu_t c_p}{k_t}$
q	energy transfer due to conduction
q_r	energy transfer due to radiation
r	recovery factor (Eq. 3-26)
R	perfect gas constant
R_d	Reynolds number based on d
R_x	Reynolds number based on x = $\frac{\rho_e u_e x}{\mu_e}$
R_ξ	Reynolds number based on ξ = $\frac{\rho_e u_e \xi}{\mu_e}$
R_θ	Reynolds number based or θ = $\frac{\rho_e u_e \theta}{\mu_e}$
Sc	Schmidt number = $\frac{\mu}{\rho D}$
Sc_t	turbulent Schmidt number = $\frac{\mu_t}{\rho D_t}$
St	Stanton number for heat transfer (Eq. 3-25)
St_o	St evaluated in the absence of mass transfer
St'	Stanton number for mass transfer (Eq. 3-32)
t	static temperature
t_r	recovery temperature for the main stream (Eq. 3-26)
t^o	stagnation temperature

T_{sat} saturation temperature for the liquid coolant which corresponds to the static pressure p

u streamwise component of velocity

u^+ dimensionless velocity (Eq. 2-5)

v normal component of velocity

W^+ dimensionless liquid flow rare (Eq. 2-10)

W_i^+ see Equation 2-37

x distance downstream from the effective leading edge of the dynamic boundary layer

y distance normal to the wall or the liquid film surface

y^+ dimensionless normal coordinate (Eq. 2-6)

Greek

Δ dynamic boundary layer thickness

Δ_c diffusional boundary layer thickness

Δ_t thermal boundary layer thickness

Δ^* displacement thickness (Eq. 4-13)

β heat transfer parameter (Eq. 3-1)

γ specific heat ratio

δ viscous sublayer thickness

δ_f liquid film thickness

δ^+ dimensionless viscous sublayer thickness

δ_f^+ dimensionless liquid film thickness (Eq. 2-11)

η_s stability effectiveness (Eq. 2-38)

θ momentum thickness (Eq. 4-14)

μ dynamic viscosity

ν	kinematic viscosity
ξ	energy thickness (Eq. 3-36)
ρ	density
τ	shear stress
$\tau_{s,o}$	wall shear stress for zero mass transfer
ϕ	energy balance parameter (Eq. 3-30)

Subscripts

o	evaluated at the plane of liquid coolant injection
1	evaluated at the terminus of the liquid-film-cooled length
2	evaluated at the terminus of the gas-vapor-cooled length
aw	adiabatic wall
d	diffusional component
e	main-stream state
g	main-stream gas
gv	gas-vapor cooling
l	liquid
L	evaluated at the gas-liquid interface but in the liquid phase
lf	liquid-film cooling
s	evaluated at the gas-liquid interface
	evaluated at the gas-liquid interface but in the gas phase
t	transpiration cooling
t	turbulent contribution
v	vapor
w	wall
	evaulated at y =

* evaluated at the reference state defined by Eqs. 3-28 and 3-29

Superscripts

o stagnation conditions

APPENDIX B

A SAMPLE CALCULATION FOR THE INTERFACE TEMPERATURE

To illustrate the manner in which the calculated results presented in Fig. 3-2 were obtained, a sample calculation for the interface temperature t_s is presented below.

For the flow conditions presented in Fig. 3-2, Eq. 3-33 reduces to the form

$$c_{p_{air}} \frac{\Delta H_v}{(t_e - t_s)} = \frac{R_v}{R_g} \left(\frac{p - p_{v,s}}{p_{v,s}}\right)$$

$$= \frac{83.35}{53.35} \left(\frac{p - p_{v,s}}{p_{v,s}}\right)$$

$$= 1.562 \left(\frac{p - p_{v,s}}{p_{v,s}}\right) \qquad \text{(B-1)}$$

Solving Eq. B-1 for the partial pressure of the vapor at the interface, one obtains

$$p_{v,s} = \frac{p}{\frac{1}{1.562} \frac{\Delta H_v}{c_{p_{air}} (t_e - t_s)} + 1} \qquad \text{(B-2)}$$

For purposes of illustration, assume that

$t_e = 2000$ R ($c_{p_{air}} = 0.2772$ B/lb)

$p = 500$ psia

For trial case, Eq. B-2 reduces to

$$p_{v,s} = \frac{500}{\frac{(2.242)\ (\Delta H_v)}{(2000 - t_s(R))} + 1} \text{ psia} \qquad \text{(B-3)}$$

To initiate the trial-and-error calculations, assume that t_s = 400F = 860R (the accuracy of the first approximation for t_s is not critical). For t_s = 960°R, the data in Ref. 33 gives ΔH_v = 826.0 B/lb and $p_{v,s}$ = 247.3 psia. Substituting those data into Eq. B-3, one obtains

$$247.3 \text{ psia} \stackrel{?}{=} \frac{500}{1.624 + 1} \text{ psia}$$

$$\neq 190.5 \text{ psia}$$

For the second calculation, assume that $p_{v,s}$ = 190.5 psia. Corresponding to $p_{v,s}$ = 190.5 psia, the data in Ref. 33 gives ΔH_v = 846.7 B/lb and t_s = 837.6R. Substituting those data into Eq. B-3, one obtains

$$190.5 \text{ psia} \stackrel{?}{=} \frac{500}{1.633 + 1} \text{ psia}$$

$$\neq 189.9 \text{ psia}$$

Continuing that procedure, assume for the next calculation that $p_{v,s}$ = 189.9 psia. Corresponding to $p_{v,s}$ = 189.9 psia, the data in Ref. 33 gives ΔH_v = 846.9 B/lb and t_s = 377.4F = 837.4R. Substituting those data into Eq. B-3, one obtains

$$189.9 \stackrel{?}{=} \frac{500}{1.633 + 1} + 1 \text{ psia}$$

$$= 189.9 \text{ psia}$$

Thus, for t_s = 2000 R and p = 500 psia, and for the flow conditions presented in Fig. 3-2, the calculated value of the temperature at the gas-liquid interface is t_s = 377.4F = 837.4R.

UNCLASSIFIED

Security Classification

DOCUMENT CONTROL DATA - R&D

(Security classification of title, body of abstract and indexing annotation must be entered when the overall report is classified)

1 ORIGINATING ACTIVITY (Corporate author) Jet Propulsion Center, Purdue University, School of Mechanical Engineering, Lafayette, Indiana	2a. REPORT SECURITY CLASSIFICATION Unclassified 2b. GROUP

3 REPORT TITLE

Liquid-film Cooling, Its Physical Nature and Theoretical Analysis

4 DESCRIPTIVE NOTES (Type of report and inclusive dates)

Interim report

5 AUTHOR(S) (Last name, first name, initial)

Gater, R. A., L'Ecuyer, M. R., and Warner, C. F

6 REPORT DATE	7a. TOTAL NO. OF PAGES	7b. NO. OF REFS
October 1965	108	54

8a. CONTRACT OR GRANT NO.	9a. ORIGINATOR'S REPORT NUMBER(S)
Nonr 1100(21) b. PROJECT NO.	TM-65-6
c. d.	9b. OTHER REPORT NO(S) (Any other numbers that may be assigned this report)

10 AVAILABILITY/LIMITATION NOTICES

Copies may be obtained from DDC or the Jet Propulsion Center, Purdue University.

11 SUPPLEMENTARY NOTES	12 SPONSORING MILITARY ACTIVITY
	Power Branch, Office of Naval Research, Washington, D. C. 20360

13 ABSTRACT A discussion of the physical nature of liquid-film cooling is presented that gives special emphasis to those phenomena occurring at the gas-liquid interface. The interfacial mass and heat balances are discussed in detail together with the phenomena of film instability and the entrainment of liquid by the gas stream. Calculated results are presented that are noted to agree favorably with the limited experimental data.

A heat transfer analysis is presented for the wall region downstream of the liquid film. That analysis is based on a relatively simple flow model, and is applicable to the case where the gas flow is compressible and subject to the influence of a streamwise pressure gradient. Two wall conditions are considered: (a) the case where the wall is adiabatic; and (b) the case where the wall is cooled externally.

DD FORM 1 JAN 64 1473

Security Classification

14. KEY WORDS	LINK A		LINK B		LINK C	
	ROLE	WT	ROLE	WT	ROLE	WT
Liquid-film cooling Cooling of rocket motors Nozzle cooling Liquid film-gas interface						

INSTRUCTIONS

1. ORIGINATING ACTIVITY: Enter the name and address of the contractor, subcontractor, grantee, Department of Defense activity or other organization *(corporate author)* issuing the report.

2a. REPORT SECURITY CLASSIFICATION: Enter the overall security classification of the report. Indicate whether "Restricted Data" is included. Marking is to be in accordance with appropriate security regulations.

2b. GROUP: Automatic downgrading is specified in DoD Directive 5200.10 and Armed Forces Industrial Manual. Enter the group number. Also, when applicable, show that optional markings have been used for Group 3 and Group 4 as authorized.

3. REPORT TITLE: Enter the complete report title in all capital letters. Titles in all cases should be unclassified. If a meaningful title cannot be selected without classification, show title classification in all capitals in parenthesis immediately following the title.

4. DESCRIPTIVE NOTES: If appropriate, enter the type of report, e.g., interim, progress, summary, annual, or final. Give the inclusive dates when a specific reporting period is covered.

5. AUTHOR(S): Enter the name(s) of author(s) as shown on or in the report. Enter last name, first name, middle initial. If military, show rank and branch of service. The name of the principal author is an absolute minimum requirement.

6. REPORT DATE: Enter the date of the report as day, month, year, or month, year. If more than one date appears on the report, use date of publication.

7a. TOTAL NUMBER OF PAGES: The total page count should follow normal pagination procedures, i.e., enter the number of pages containing information.

7b. NUMBER OF REFERENCES: Enter the total number of references cited in the report.

8a. CONTRACT OR GRANT NUMBER: If appropriate, enter the applicable number of the contract or grant under which the report was written.

8b, 8c, & 8d. PROJECT NUMBER: Enter the appropriate military department identification, such as project number, subproject number, system numbers, task number, etc.

9a. ORIGINATOR'S REPORT NUMBER(S): Enter the official report number by which the document will be identified and controlled by the originating activity. This number must be unique to this report.

9b. OTHER REPORT NUMBER(S): If the report has been assigned any other report numbers *(either by the originator or by the sponsor)*, also enter this number(s).

10. AVAILABILITY/LIMITATION NOTICES: Enter any limitations on further dissemination of the report, other than those imposed by security classification, using standard statements such as:

(1) "Qualified requesters may obtain copies of this report from DDC."

(2) "Foreign announcement and dissemination of this report by DDC is not authorized."

(3) "U. S. Government agencies may obtain copies of this report directly from DDC. Other qualified DDC users shall request through

_____."

(4) "U. S. military agencies may obtain copies of this report directly from DDC. Other qualified users shall request through

_____."

(5) "All distribution of this report is controlled. Qualified DDC users shall request through

_____."

If the report has been furnished to the Office of Technical Services, Department of Commerce, for sale to the public, indicate this fact and enter the price, if known.

11. SUPPLEMENTARY NOTES: Use for additional explanatory notes.

12. SPONSORING MILITARY ACTIVITY: Enter the name of the departmental project office or laboratory sponsoring *(paying for)* the research and development. Include address.

13. ABSTRACT: Enter an abstract giving a brief and factual summary of the document indicative of the report, even though it may also appear elsewhere in the body of the technical report. If additional space is required, a continuation sheet shall be attached.

It is highly desirable that the abstract of classified reports be unclassified. Each paragraph of the abstract shall end with an indication of the military security classification of the information in the paragraph, represented as *(TS)*, *(S)*, *(C)*, or *(U)*.

There is no limitation on the length of the abstract. However, the suggested length is from 150 to 225 words.

14. KEY WORDS: Key words are technically meaningful terms or short phrases that characterize a report and may be used as index entries for cataloging the report. Key words must be selected so that no security classification is required. Identifiers, such as equipment model designation, trade name, military project code name, geographic location, may be used as key words but will be followed by an indication of technical context. The assignment of links, roles, and weights is optional.